Response to Reviewer #1

The authors have greatly improved the manuscript responding to the two reviewers' comments. I believe this paper is suitable for publication after minor revisions.

Largest minor points:

Line 28-30: Include the boxed regions shown on Figure 3a,c on the other figures of Eastern China ozone (e.g., Figure 1, 4, 7, 8) to assist the reader throughout the manuscript. Then here when you list the location of these regions the authors can reference Figure 1b.

Reply:

According to the features of each Figure, the mentioned boxes were also included in Figure 1, 4, 7 and 8.

When we listed the locations, e.g., NC, YRD and PRD, Figure 1b was referenced.

Revision:

……the high O_3 concentrations in China are mainly observed in urban regions, such as in North China (NC, Figure 1b), the Yangtze River Delta (YRD) and the Pearl River Delta (PRD) where rapid……

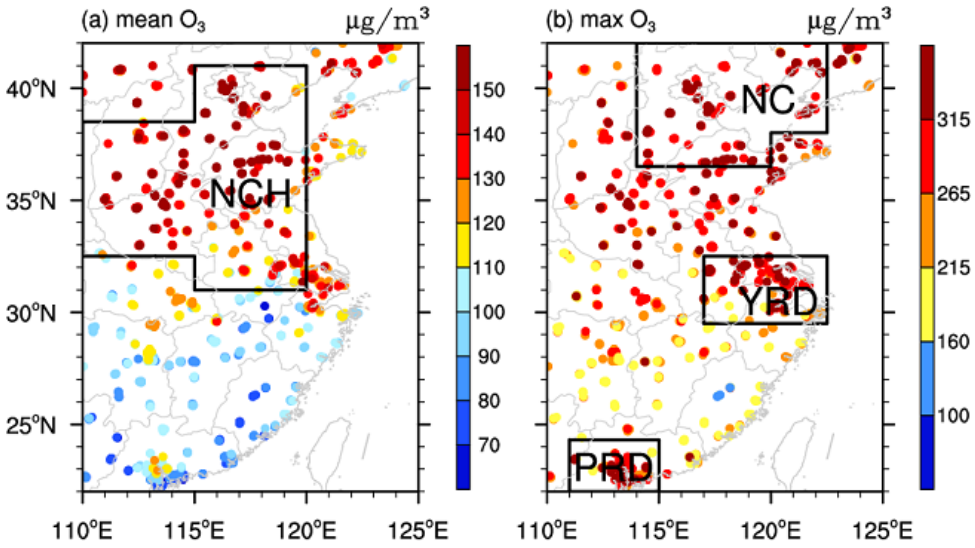

Figure 1. Distribution of the (a) mean values and (b) maximum values of MDA8 (Unit: μg/m³) at the observation sites in summer from 2015 to 2018. The black boxes in panels a and b indicated the locations of North China and Huanghuai region (NCH), North China (NC), Yangtze River Delta (YRD) and Pearl River Delta (PRD).

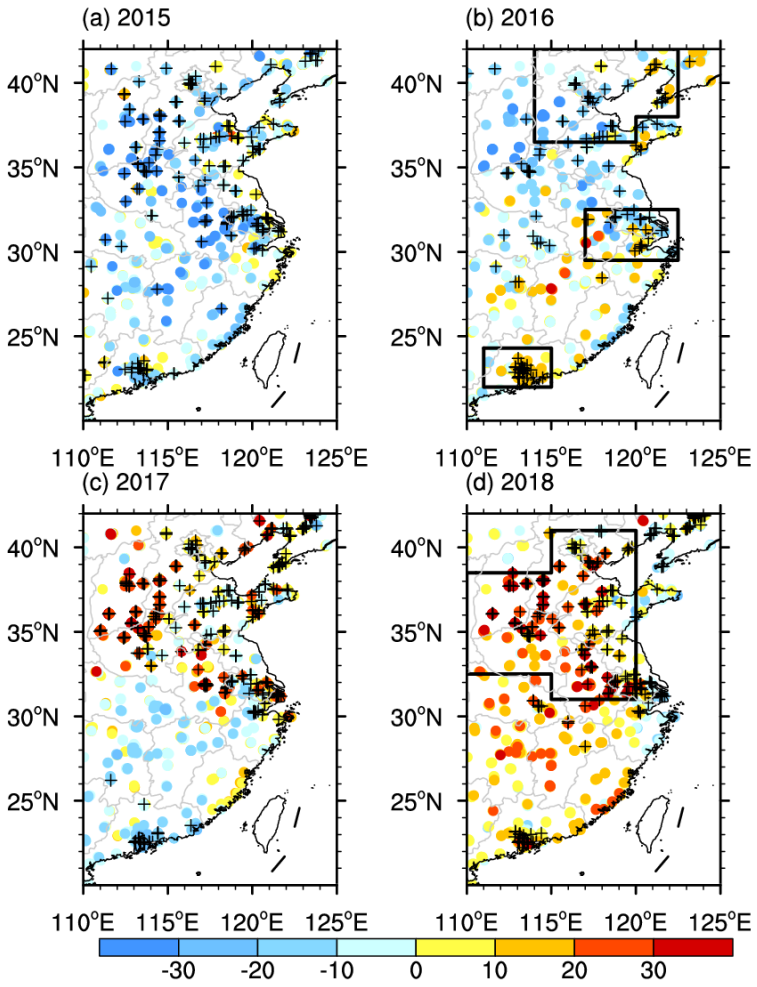

Figure 2. Anomalies of the summer mean MDA8 (Unit: μg/m³) in 2015 (a), 2016 (b), 2017 (c) and 2018 (d), relative to the mean during 2015–2018. The black pluses indicate that the maximum MDA8 was larger than 265 μg/m³. The black boxes in panel b indicated the locations of NC, YRD and PRD, while that in panel d was the NCH area.

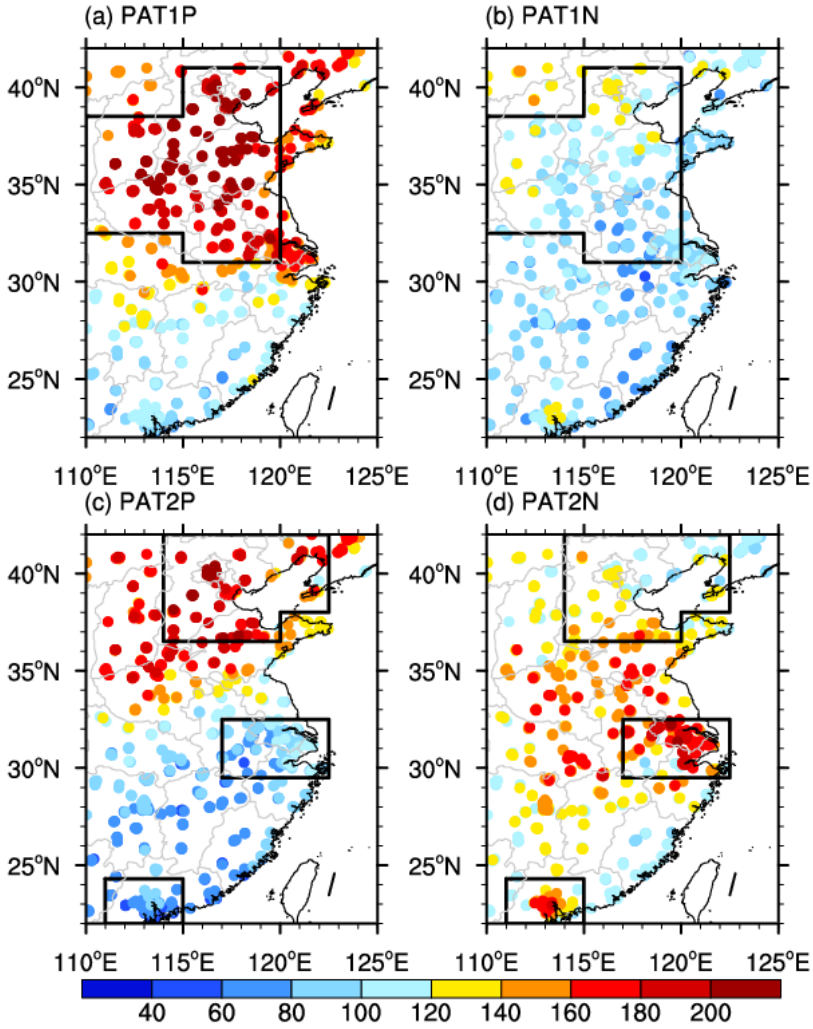

Figure 5. Composites of the MDA8 (Unit: μg/m³) for PAT1 (a, b) and PAT2 (c, d) in summer from 2015 to 2018. Panels (a) and (c) were composited when the time coefficient of EOF1 and EOF2 was greater than one standard deviation, while panels (b) and (d) were composited when the time coefficient was less than –1×one standard deviation. The black box in panel a-b indicated the location of NCH, while those in panel c-d were the NH, YRD and PRD area.

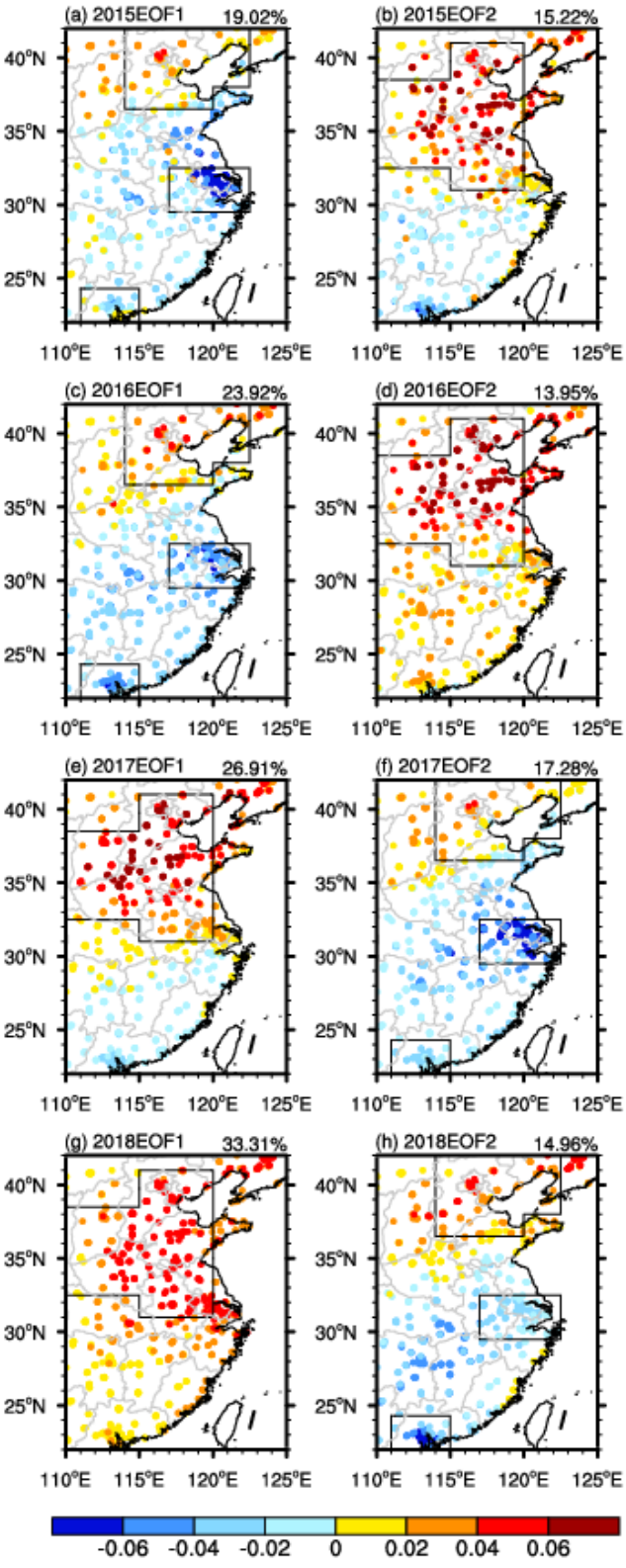

Figure 8. The first (a, c, e, g) and second (b, d, f, h) EOF spatial patterns of MDA8 in summer in 2015 (a, b), 2016 (c, d), 2017, (e, f) and 2018(g, h). The percentage number in panels (a, c, e, g) and (b, d, f, h) are the variance contributions of the first and second EOF mode. The black boxes indicated the location of NCH, NH, YRD and PRD, respectively.

Line 111: Do you think the high levels of MDA8 around the large cities has to do with aged pollutant transport in the cities, which may be related to lower O3 in the cities due to NOx titration but outside of the cities the air was in a different NOx regime and O3 increased? This idea has been largely absent from this paper, but I believe it is worth discussing.

Reply:

The related discussions were added in the revised manuscripts, e.g., in the Introduction, the first paragraph of Section 3, and in the Conclusions and Discussions.

Revision in the Introduction:

……Although deep stratospheric intrusions may elevate surface ozone levels (Lin et al., 2015), the main source of surface ozone is the photochemical reactions between the oxides of nitrogen (NO_x) and volatile organic compounds (VOC), i.e., NO_x + VOC = O_3. The concentrations of NO_x and VOC are fundamental drivers impacting ozone production, and are sensitive to the regime of ozone formation, i.e., NO_x-limited or VOC-limited (Jin and Holloway 2015)……

Revision in the first paragraph of Section 3:

……Surface O_3 pollution was closely linked to the anthropogenic emissions that dispersed and concentrated in the large cities (Fu et al., 2012), which was similar to the haze pollution (Yin et al., 2015). In the megacity cluster, the photochemical regime for ozone formation is combination of NO_x-limited and VOC-limited regimes (Jin and Holloway 2015). In the YRD and PRD, high levels of MDA8 were scattered around the large cities. Due to high emissions of NO_x both in large and small cities in the NCH region, the high-level O_3 values were contiguous, indicating extensively surface O_3 pollution (Figure 1)……

Revision in the Conclusions and Discussions:

……In this study, we mainly emphasized the contribution of the meteorological impacts and assumed the emissions of ozone precursors were relatively stable on the daily time-scale. Observational and modelling studies suggested that photochemical production of ozone in the NC, YRD and PRD was the transitional regime (i.e., both

reductions of NO_x and VOC would reduce O_3), which would influence the concentrations of surface ozone (Jin and Holloway 2015). There is no doubt that the human activities were the fundamental driver of air pollution even on the daily time-scale, thus the joint effects of the daily meteorological conditions and anthropogenic emissions (including the photochemical regimes) needed to be discussed in future work……

Line 116: Severe O3 pollution is mentioned a few times in the paper but "severe" is not defined as a threshold. What do the authors mean by this? Is it anything above "Moderately polluted"?

Reply:

Most of the uses of "severe" were replaced by more accurate presentations, such as "high levels of O_3 pollutions", "heavily polluted O_3 pollutions" and "high concentrations of O_3", etc.

Revision :

Shanghai in YRD, Guangdong and Zhongshan in PRD (Figure S2). These cities had large populations and were with ~~severe~~ high levels of O_3 pollutions. In Beijing, Tianjin and Tangshan, the MDA8 values were nearly above 100 μg/m³ and frequently

distribution of the mean MDA8, the maximum MDA8 to the south of 30°N was lower by comparison. Although approximately 60% of summer days were non-O_3-polluted in the cities of Guangzhou and Zhongshan (Figure 2d), heavily polluted ~~severe~~ O_3 pollution also occurred in the PRD (Figure 1b). ↵

and <120 μg/m³ for PAT1P and PAT1N, respectively. For the second pattern, the PAT2P appeared as a diminishing pattern from the north to the south (Figure 4c), however, there was ~~severe~~ high concentrations of ozone pollution in the YRD and PRD under PAT2N conditions (Figure 4d). Therefore, the centres of O_3 variation were NCH for the PAT1, and NC and the YRD for

Line 139: The authors focus the discussion of PAT2 on NC and YRD, with the occasional mention to PRD (e.g., line 207-208). Often there are places where the comment applies to both YRD and PRD (e.g., Lines 146, 181-202) and could be included. Is there a reason why not to include it in the discussion of PAT2?

Reply:

From the mean MDA8 (Figure 1a), the composites for PAT2 (Figure 4), the ozone concentrations in PRD were not as high as those in the NC and YRD areas. Thus, we did not pay much attentions on PRD region. Particularly, in the "Associated atmospheric circulations", we did not mention the ozone pollution in PRD.

However, when analyzing the observational features, we also included the ozone in PRD to show some new features.

Lines 223-251: I am not convinced by the discussion of Figures 10 and 11 as this is one year being compared to a really small sample size of a four-year average which includes that same one year. It is the nature of the availability of the data that the authors choose not to extend their analysis further back. I think the paper can stand alone without these two additional figures and discussion. This could be revisited after more time has passed in a later publication.

Reply:

According to the reviewer's comment, we decided to cancel the Figure 10 and 11. We now focus on the dominant patterns and their varying features in different years. Some new works will be supplemented and we will revisit the Figure 10 and Figure 11 in a later manuscript.

The contents related to Figure 7–9 were rewritten and redistributed in the revised version. The texts associated Figure 10 &11 were deleted. Detailed revisions can be found in the revised manuscript and also the mark-up manuscript.

Minor and technical comments:

Line 22: Start off the first sentence with something like "High levels of ozone occur both in the stratosphere and at the ground level". Otherwise ozone occurs throughout the troposphere, just not always at unhealthy concentrations.

Reply:

According to the reviewer's comment, this sentence was revised.

Revision:

High levels of ~~O~~ozone occurs both in the stratosphere and at the ground level. Stratospheric ozone forms a protective layer at shields us from the sun's harmful ultraviolet radiation. However, surface ozone is an air pollutant and has harmful effects

Line 34: I do not understand the significance of the greater ozone trend on the highest mountain in NC. This indicates to me that the background ozone in the free troposphere in the region is possibly increasing. Is this what the authors mean? Please clarify the significance of this statement.

Reply:

What we meant is that the increasing trend was widespread in the east of China and it is meaningful to study the variations in ozone pollution in this region. Furthermore, after your reminder, we thought the increasing trend partly indicate the background ozone in the free troposphere in the region is possibly increasing.

Referencing the reviewer's suggestion, we revised the statement as follows.

Revision:

……Although far away from the anthropogenic emissions, the summer (June-July-August, JJA) O_3 on the highest mountain over NC (Mount Tai) increased significantly by 2.1 ppbv yr^{-1} from 2003 to 2015 (Sun et al., 2016)……

Line 44: I believe the Li et al. paper (note, add the period after 'al' in this sentence. It is missing. Check all references for this) uses the GEOS-Chem CTM, not the GEOS CTM. These are different models.

Reply:

We referenced the name of the model used by Li et al. (2018) in their Abstract.

rural NO_x-limited conditions. However, simulations with the Goddard Earth Observing System Chemical Transport Model (GEOS-Chem) indicate that a more important factor for ozone trends in the North China Plain is the ~40% decrease of fine particulate matter ($PM_{2.5}$) over the 2013–2017 period, slowing down the aerosol sink of hydroperoxy (HO_2) radicals and thus stimulating ozone production.

After carefully checking their publication, we found the detailed name of the model in the Mechods. The sentence was revised as follows:

Revision:

……Employed the GEOS-Chem chemical transport model, Li et al. (2018) found that rapid decreases in fine particulate matter levels significantly stimulated ozone production in NC by slowing down the aerosol sink of hydro-peroxy radicals……

Line 57: Can the authors provide a summary sentence at the end of this paragraph linking all these studies together?

Reply:

According to the reviewer's comment, a summary sentence was supplemented.

Revision:

……Thus, in addition to human activities and secondary aerosol processes, the impacts of atmospheric circulations and meteorological conditions must be systematically studied to improve understanding of the O_3 pollution in North China……

Line 58-59: The authors claim that Wang et al. (2017) claim the study uses ozone data from prior to 2010. How can the reader then assume that the 7 referenced studies in the paragraph above with publication dates prior to 2019 are using recent enough ozone data to that the authors can use these papers to make their claims?

Reply:

To avoid the confusions, we deleted this sentence.

Revision:

~~Wang et al. (2017) reviewed the meteorological influences on ozone events, but the referenced findings were published mainly before 2010, when measurements in China were still scarce.~~ Since 2015, O_3 measurements in eastern China were

Line 62: I know I asked how your study is different to the Zhao and Wang (2017) paper, but stating "Actually, in our study, we found the …." comes out of nowhere compared to the rest of your introduction. Please modify this sentence to be less aggressive and more like, "In this study, we built upon the previous literature

analyzing ozone and meteorological influences thanks to the availability of more ozone observations by the Chinese government since 2015, providing us more information to analyze then available in these earlier studies, e.g., Zhao and Wang (2017).”

Reply:

Thanks to the kind remind from the reviewer. We worried too much to show the differences between our studies and Zhao and Wang (2017) and now follow the reviewer’s suggestions.

Revision:

The dominant patterns of daily ozone in summer in east of China are still unclear. In this study, we built upon the previous literature analysing ozone and meteorological influences thanks to the availability of more ozone observations by the Chinese government since 2015, providing us more information to analyse than available in these earlier studies, e.g., Zhao and Wang (2017).

Line 73: What threshold was used to unify the sites? For example, did some sites move location but still considered as one time series?

Reply:

The sites with missing data >5% were removed and there were 868 sited were kept in the four years.

Line 80: Thank you for adding this detail. However, I am not used to this type of notation; is there a reason some left brackets are curved (and not [?

Reply:

It is accurate mathematical notations. That is, [contained the boundary value, however, (did not contained it.

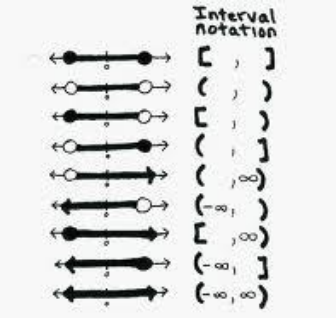

Line 82: Can you provide a link either here in the text or at the end of the paper in a "Data Availability" section to where you got the ERA-Interim data.

Reply:

Data Availability was added as the ACP journal required.

Revision:

Data availability.

Hourly O_3 concentration data is supported by the website: http://beijingair.sinaapp.com (Ministry of Environmental Protection of China, 2018). Atmospheric circulation datasets are downloaded from http://www.ecmwf.int/en/research/climate-reanalysis/era-interim (ERA-Interim, 2018).

Line 83: Remove at to read "temperature from surface to 100 hPa".

Reply:

The errors were corrected.

Revision:

air temperature ~~at~~ from surface to 100 hPa,

Line 86, 89-90: (1) I am still confused by this description of reanalysis timesteps to Beijing time. How many 6-hourly reanalysis timestamps are used in the daytime data analysis? Why are there different time period for the 3-hourly data than 6 hourly data? Can you use the same time period but just more 3-hourly data?
(2) 00 am to 00pm UTC does not make sense. I think you mean 00 UTC to 12 UTC which would mean you have 3 6-hourly timesteps (00, 06, 12 UTC). The am and pm should also be removed from the 21 UTC to 09 UTC. And this means you have 5 3hourly timesteps (21, 00, 03, 06, 09 UTC). Why is this offset 3 hours from the 6-hourly timesteps (could have done 00,03,06,09, 12 UTC)?

Reply:

(1) The required answers were clearly shown on the website of ERA-Interim (https://confluence.ecmwf.int/pages/viewpage.action?pageId=56658233). On the page

about “ERA-Interim: 'time' and 'steps', and instantaneous, accumulated and min/max parameters”, we can found the explanations about the parameters.

ERA-Interim data is archived at website differently according to whether they are produced by the **analysis (An), or the forecast (Fc)**, and timesteps of data which we could get is shown in Fig R1. Only precipitation and surface solar are produced by forecast in all the data which we used, which was illustrated in Table 8 and 9 of Berrisford et al. (2011). Fc data is the **accumulated** (from the beginning of the forecast) and can be treated as 3-hr data due to 4 timesteps in 12 hours, and An data is **instantaneous** (Berrisford et al., 2011).

We wanted to research the link between atmospheric circulation and MDA8 which mostly occurs in daytime (8:00 a.m. to 8:00 p.m. Beijing Time). For Fc, we considered **00 UTC to 12UTC (8:00 to 20:00 Beijing Time)**, the upper way in Figure R1, (first ‘+12’ line in Fig. R1) as daytime in Beijing. It means we just use 1 timesteps data which is accuunulated from 00 UTC to 12 UTC. But for An (second line in Fig. R1), we could only calculate the mean of 00:00 and 06:00 UTC as daytime mean and it represent mean of the time-scale 3-hour (half of the timesteps) before the 00:00 to 3-hour after 06:00. It means that daytime is **21 UTC to 9 UTC (5:00 to 17 Beijing Time).**

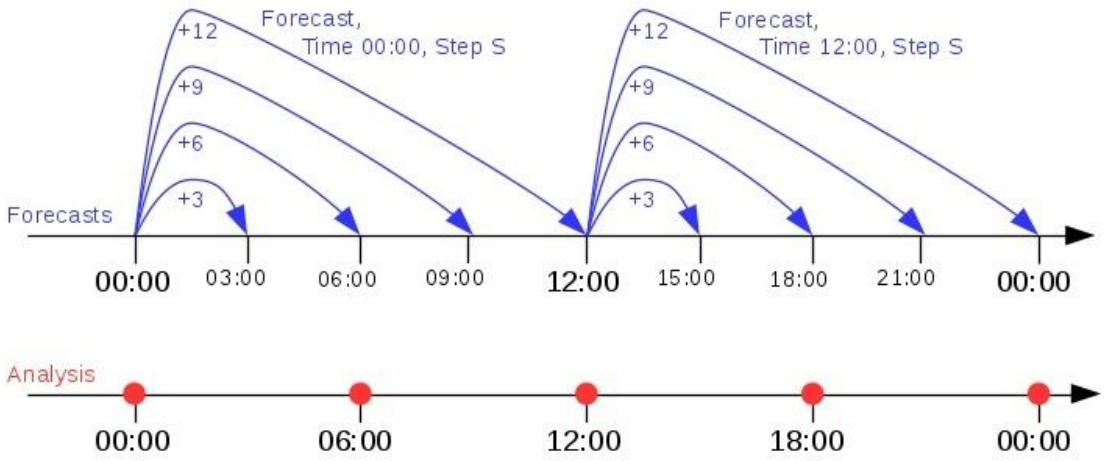

Figure R1. ERA-interim Data timesteps (downloaded from the ERA website).

Reference:

Berrisford, P, Dee, DP, Poli, P, Brugge, R, Fielding, M, Fuentes, M, Kållberg, PW, Kobayashi, S, Uppala, S, Simmons, A, The ERA-Interim archive Version 2.0. https://www.ecmwf.int/node/8174.

(2) The timing way was changed to 24HR way.

Revision:

……Due to the different representative period of each element in ERA-Interim data, the daytime for Z, wind, relative humidity, vertical velocity, air temperature and cloud cover was from 05 to 17 (Beijing Time; 21–09 UTC), while it is from 08 to 20 (Beijing Time; 00 to 12 UTC) for precipitation and downward solar radiation……

Line 94: remove 'ly' from relatively

Reply:

The errors were corrected.

Revision:

extracted the relative~~ly~~ change features of the original data on the daily time-scale.

Line 104: I suggest changing this sentence to "….was mostly lower than 100 ug/m3, and lower than the O3 pollution in North China and in the Huanghuai area (NCH, about 31-41N, 110-120E)". This modifies the second half of the sentence as well as adding in the box region for the NCH (which I guessed from Figure 3).

Reply:

The errors were corrected.

Revision:

South China), the mean MDA8 was mostly lower than 100 μg/m³ and ~~the ozone pollution was obviously~~ lower than ~~that~~ the O_3 pollution in North China and in the Huanghuai area (NCH, Figure 1a). It is notable that, although the values of MDA8 in the

Line 112: are cities large and small based on population or area-covered?

Reply:

The large and small cites are distinguished based on population.

Line 115: Could highlight that this threshold is matching the list now given in line 80-81; e.g., change to ….the threshold of "heavily O3 pollution" in China…

Reply:

According to the reviewer's advice, this sentence was improved.

Revision:

Furthermore, the maximum values of MDA8 for four summers were extracted to evaluate the severest levels of O_3 pollution (Figure 1b). To the north of 30°N, the maximum MDA8 at most sites was above 265μg/m³ (i.e., the threshold of heavily O_3 pollution in China), indicating that ~~the levels of~~ heavily O_3 pollution had occurred. ~~exceeded the threshold of heavily O_3 pollution in China (The Ministry of Environmental Protection of China, 2012).~~ The observed summer MDA8 anomalies in

Line 118: Are these cities with large populations "Megacities"?

Reply:

Yes, these cities with large populations are megacities. To emphasize the large populations, we maintained the presentation.

Line 119: How often was the MDA8 value nearly above 100 ug/m3? Are you trying to say the ozone was hardly below 100 ug/m3 on any day in the time series?

Reply:

The detailed percentages were explained in the next sentence.

The percentage of non-O_3-polluted days (<100 μg/m³) and moderate O_3-polluted days (>215 μg/m³) were 14.9% and 15.5% for the mean MDA8 of these three cities.

Line 122: What does "exceeded the health threshold" in reference to? Is that "Good" and above?

Reply:

It is the upper limit "Excellent" level.

Revision:

μg/m³) were 14.9% and 15.5% for the mean MDA8 of these three cities. The former percentage indicated that more than 85% O_3 concentrations exceeded the health threshold (i.e., the upper limit "Excellent" level), and the later meant, in more than 15%

Line 127: Change reference to (Figure 2a,b)

Reply:

The sentence was corrected.

Revision:

to those of Beijing and Tianjin in 2017 and 2018 (Figure ~~2~~3a, b). In Nanjing and Shanghai, the MDA8 did not show a clear increasing trend (Figure ~~2~~3c). Similar to the distribution of the mean MDA8, the maximum MDA8 to the south of 30°N was

Line 141: There looks to be extra spacing in front of -1x

Reply:

The errors were corrected.

Revision:

……less than –1 ×one standard deviation…..

Line 142: Change showed to shows. There are other places where the authors switch back and forth between verb tenses (e.g., Line 154, 159).

Reply:

Similar errors were checked and corrected throughout the manuscript.

Line 145: add (Fig 4a, b) after "respectively".

Reply:

The reference of Figure were added.

Revision:

and <120 μg/m³ for PAT1P and PAT1N, respectively (Figure 5a, b). For the second pattern, the PAT2P appeared as a diminishing pattern from the north to the south (Figure 45c), however, there was ~~severe~~ high concentrations of ozone pollution

Line 149: change recent four years to "the four years of study" since this becomes less true after publication.

Reply:

The errors were corrected.

Revision:

In eastern China, the economic productions and human actives steadily developed in the ~~recent~~ four years of study and the emissions of ozone precursors were reasonably supposed to be relatively stable on the daily time-scale. Differently, the daily

Line 150: What does "were reasonably supposed to be relatively stable on the daily time-scale" mean. I think change to "Despite the economic productions and human activities steadily increasing from 2015 to 2018 in Eastern China, we assume the emissions of ozone precursors to be relatively stable on the daily time-scale".

Reply:

According to the reviewer's advice, this sentence was improved.

Revision:

In eastern China, despite the economic productions and human actives steadily increased in the four years of study and we assume the emissions of ozone precursors to be relatively stable on the daily time-scale.

Line 154-156: I do not feel this "For example," sentence is necessary.

Reply:

This sentence was deleted.

Revision:

(PAT2P composite minus PAT2N composite) ~~were~~ are shown Figure ~~5~~6–~~6~~7. ~~For example, the mean of the atmospheric circulations associated PAT1P (PAT1N) were firstly computed, and then the differences between PAT1P composites and PAT1N composites were calculated as the anomalous daytime atmospheric circulations associated with PAT1.~~ For the first

Line 158: so this is stagnation and as such there is the buildup of pollutants too without removal from weather systems passing by. I do not think that idea has been discussed.

Reply:

The removal of ozone pollutants by the weather were clearly discussed in the revised manuscript, which make our study more complete.

Revision in the Abstract:

western ridge point shifted northward. The local hot, dry air and intense solar radiation enhanced the photochemical reactions to elevate the O_3 pollution levels in North China and Huanghuai region, however the removal of pollutants were decreased. For

Revision in Section 4:

coefficient between the time series of PAT1 and the NCH-averaged MDA8 was 0.97 (Table 1). Thus, the effects of the anomalous atmospheric circulations mainly acted on the photochemical reactions near the surface in NCH and the removal of pollutants. In Figure 6a, ~~T~~there were negative Z850 anomalies over the Ural Mountains. Over the broad region from eastern ~~5~~6a), less precipitation (Figure ~~5~~6b), a dry environment (Figure ~~5~~6c) and intense solar radiation (Figure ~~5~~6d), which substantially enhanced the generation of ozone in NCH but weakened the removal of the pollutants.

For PAT2, largest O_3 differences (PAT2P composite minus PAT2N composite) were observed in the NC and YRD regions (Figure ~~3~~4c, Figure 45c, d). The correlation coefficient between the time series of PAT2 and the MDA8 difference between NC and the YRD was 0.77 (Table 1). The impacts of atmospheric circulations on the photochemical reactions and removal effects in the above two areas are analysed in Figure ~~6~~7. Due to the broad positive Z500 anomalies at the high latitudes cover over NC, resulting in dry, hot and sunny weather (Figure ~~6~~7b, d). Under such meteorological conditions, the generation of surface O_3 was accelerated but the removal processes were slowed down, and thus, higher MDA8 was observed in NC. The

Revision in Conclusion:

prevented the northward transportation of moisture. The northward-shifted western ridge point of the west Pacific subtropical high accelerated the photochemical reactions via hot-dry air and intense solar radiation, but weaken the removal of pollutants ~~via hot-dry air and intense solar radiation~~. The second pattern of ozone pollution showed remarkable south-north differences.

Line 159: Start sentence with "In Figure 5a, there are negative …"

Reply:

This sentence started with "In Figure 6a" now.

Revision:

pollutants. In Figure 6a, ~~T~~there were negative Z850 anomalies over the Ural Mountains. Over the broad region from eastern Eurasia to the north Pacific, the anomalous atmospheric circulations were located zonally, i.e., positive Z850 on the tropical

Line 163: Change to "(EAT, Table 1)"

Reply:

According to the reviewer's advice, this sentence was improved.

Revision:

deep trough was enhanced and extended to northeast China and Japan. The intensity of the East Asia deep trough (i.e., the negative area-averaged Z850) positively correlated with the time series of PAT1 (EAT, Table 1) with a correlation coefficient

Line 166: This final part might be a bit of a stretch.

Reply:

There is local anti-cyclonic circulation over NCH, which could prevent the cold air to arrive at the NCH region (Figure 6b).

According to the reviewer's advice, this sentence was improved.

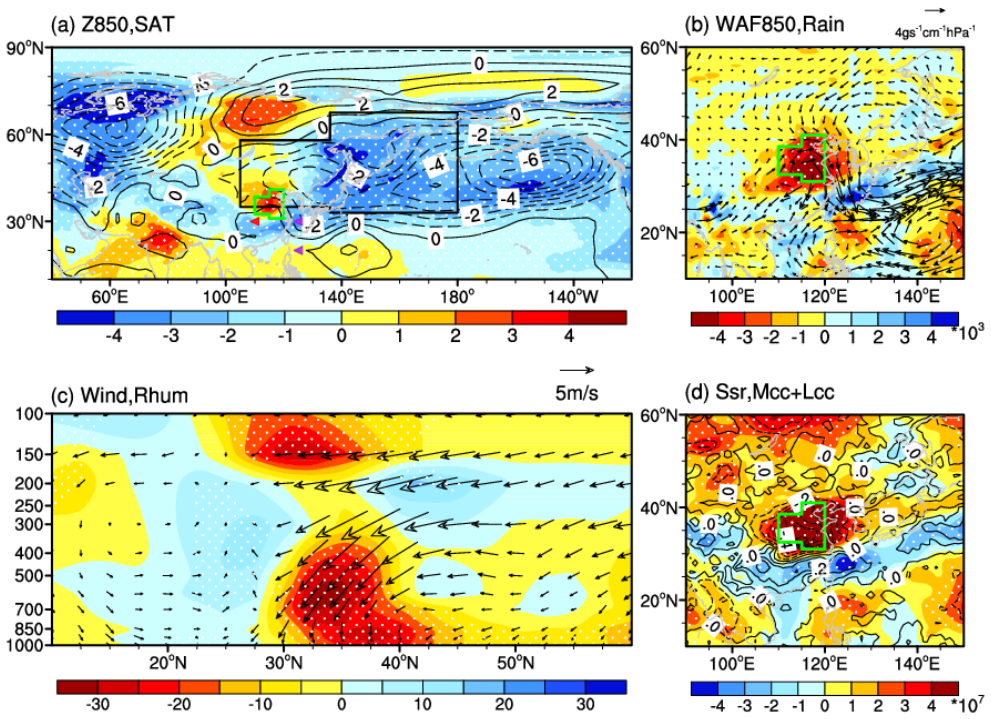

Figure 6. Differences of the daytime atmospheric circulations (i.e., PAT1P minus PAT1N). (a) Geopotential height at 850 hPa (Unit: 10gpm, contours) and surface air temperature (Unit: K, shading), (b) water vapor flux (Unit: kg*m/(kg*s)) at 850 hPa (arrows) and precipitation (Unit: mm, shading), (c) 100°E–120°E mean wind (Unit: m/s, arrows) and relative humidity (Unit: %, shading), (d) downward solar radiation at the surface (Unit:10^7 J/m^2, shading) and the sum of low and medium cloud cover (Unit: 1, contours). The white dots indicate that the shading was above the 95% confidence level. The green boxes in panels (a), (b) and (d) show the NCH region, and the black box in panel (a) indicates the location of the East Asia trough. The purple triangles in panel (a) indicated the data used to calculate the $WPSH_1$, while the red triangle represented the west ridge point of WPSH.

Revision:

……In accordance with the deep positive height anomalies to the north of Lake Baikal (centring at 107 °E, 53.5 °N), which also extended southward to the edge of the Tibetan Plateau (Figure 6a), cold air was transported to the lower latitudes. However,

local anti-cyclonic circulation over NCH prevented the cold air to arrive at the NCH region (Figure 6b).……

Line 184: In the author's comments to my first review, they explain to me why they choose different pressure levels for Figure 5a and 6a, but please include the reasoning in the paper.

Reply:

According to the reviewer's advice, related contents were included.

Revision:

between NC and the YRD was 0.77 (Table 1). The impacts of atmospheric circulations on the photochemical reactions and removal effects in the above two areas are analysed in Figure ~~6~~7. It is notable that the signals of atmospheric circulations were clearer at the lower troposphere (i.e., 850 hPa) for PAT1 (Figure 6a), however, the signals for PAT2 could be recognized both at the low- and mid- troposphere (Figure 7a). Due to the broad positive Z500 anomalies at the high latitudes of Eurasia, the

Line 186: It is really difficult to find Chukchi Peninsula on the map given the country lines are in grey. Can you include lat/lon of the region you mean because I think the peninsula is mostly under negative Z500.

Reply:

The lat/lon of Chukchi Peninsula was included.

Revision:

……from the Chukchi Peninsula (about cantering at 180 ^{o}E, 66.5 ^{o}N) to Northeast China……

Line 188: Similarly, I would argue that it was limited to the east of Korea so again add coordinates to ensure your reader is looking where you want them to be looking.

Reply:

According to the reviewer's advice, this sentence was improved.

Revision:

……The East Asia deep trough was stronger (R=0.3), but was limited to the Sea of Japan.

Line 194: Remove the word obvious.

Reply:

According to the reviewer's advice, this sentence was improved.

Revision:

YRD region (Figure 67b). A moist-cool environment, weak solar radiation and ~~obvious~~ wet deposition reduced the ozone

Line 204: Change "the past four years" to "these past four years" as this will change after publication.

Reply:

According to the largest minor comment to Figure 10 & 11, the related sentence was already deleted.

Line 217: Could include a reference to Fig 8.

Reply:

According to the largest minor comment to Figure 10 & 11, the related sentence was already deleted.

The following are the reasons why I do not think Figures 10 and 11 add to the manuscript:

Line 223: change to "were generally negative". I think there is a mix of positive and negative in the YRD in Figure 7b, not strictly positive as is written.

Line 227: Again, I see a ridge over Chukchi Peninsula, not a trough, so include coordinates of where you want the reader to be looking.

Line 229: Both Figure 10 and 11 could have the same purple arrows to identify how the authors would calculate the WPSH as in Figures 5 and 6. Again, authors could include coordinates or a box region as in Figures 5 and 6 to indicate the location of EAT and WPSH.

Line 231: I disagree with the authors that more low to mid-level clouds formed as it looks to me that the box straddles the zero line and that instead of a decrease in

solar radiation reaching the ground in NC I see positive colors in that box too in Figure 10d.

Line 236: What do the authors mean by "south of YRD"? Do they mean outside of the box or the southern portion of the YRD? Does that mean PRD?

Lines 225-237: There are no significant differences near the NC or YRD in any of the four panels in Figure 10.

Line 238: I do not like how the sentence starts with "-+-". Can the authors at least put "The" prior to the symbols? Is this the same as an OMEGA block and could be written as such instead of -+- ?

Line 243: I do not see an anomalous anticyclone over the NCH in Figure 11a, but more on the border with cyclonic flow to the southwest and anticyclone to the east, and as the authors describe later in reference to the water vapor flux, the NCH is in a region of anomalous divergent flow.

Line 244: When the authors say "it was difficult to form cloud" the NCH straddles the zero line and shows a mix of both positive and negative SSR so how can they say "more solar radiation directly reach the ground (Figure 11d)"?

Line 247: Out of nowhere the authors mention "signals of global warming". Such bold statements in a manuscript, which depend on figures in the supplemental material, should not be made.

Reply:

According to the largest minor comment to Figure 10 & 11, the related sentence was already deleted.

We now focus on the dominant patterns and their varying features in different years. Some new works will be supplemented and we will revisit the Figure 10 and Figure 11 in a later manuscript. **We believe the above comments from the reviewer will be helpful in our new researches.**

The contents related to Figure 7–9 were rewritten and redistributed in the revised version. The texts associated Figure 10 &11 were deleted. Detailed revisions can be found in the revised manuscript and also the mark-up manuscript.

Overall the Discussion is fine.

Line 254: Add a reference (e.g. Li et al., 2018) to the end of the opening sentence, possibly bringing over the point made at the end of the discussion on line 281 "At present, the fine PM decreased in the summers in eastern China…."

Reply:

According to the reviewer's advice, this sentence was improved.

Revision:

At present, the fine particulate matter decreased in the summers in eastern China, and ground-level ozone pollution became the major air challenge in the summers in the east of China (Li et al., 2018).

Line 264: the increased SAT and thus decreased cold air advection from the north a) seems backwards (less cold air advection would likely lead to increased SAT at lower latitudes) and b) the negative Z500 to the west with flow from south and southwest likely brought warmer temperatures from the southern latitudes into the region.

Reply:

According to the reviewer's advice, this sentence was improved.

Revision:

……positive geopotential height anomalies at the high latitudes significantly decreased cold air advection from the north and thus increased the surface air temperature……

Line 270: "…daily emission data were difficult to be acquired" implies the authors have acquired such data. Is that true or are these data difficult to acquire?

Reply:

It is true these are difficult to acquire. To avoid such confusions, we revised this sentence.

Revision:

……There is no doubt that the human activities were the fundamental driver of air

pollution even on the daily time-scale, thus the joint effects of the daily meteorological conditions and anthropogenic emissions needed to be discussed in future work……

Line 273: remove the comma before (2019).

Reply:

The errors were corrected.

Revision:

……Lu et al. (2019) found that……

Line 275: How were the "domestic anthropogenic emissions alone would have led to ozone decreases" determined by the Lu et al. study?

Reply:

Lu et al. (2019) based on series of GEOS-Chem experiments and gave such conclusions.

> ozone chemical production. Our results indicate that there would be no days with MDA8 ozone > 80 ppbv in these major Chinese cities in the absence of domestic anthropogenic emissions. We find that the 2017 ozone increases relative to 2016 are largely due to higher background ozone driven by hotter and drier weather conditions, while changes in domestic anthropogenic emissions alone would have led to ozone decreases in 2017. Meteorological conditions in 2017 favor natural source contributions (particularly soil NO_x and

According to the reviewer's advice, this sentence was improved.

Revision:

2017 surface ozone increases relative to 2016 in China are largely due to hotter and drier weather conditions, while changes in domestic anthropogenic emissions alone would have led to ozone decreases in 2017 basing on their GEOS-Chem experiments.

Line 277: Is "were still unclear" in reference to your work presented here or in reference to the Lu et al. study?

Reply:

According to the reviewer's advice, this sentence was improved.

Revision:

……The simultaneous large-scale atmospheric circulations on an interannual scale and their possible preceding climate drivers, e.g., sea ice, and sea surface temperature, were **still unclear so far**……

Figure comments:

Figure 2: Can NC, NCH, YRD, and PRD be added to the Figure caption in a similar fashion to how it was added to the Comments to the Reviewer (Page 47). Also, could add a reference to Figure S2 in the caption to remind readers to look there for the locations of these cities.

Reply:

According to the reviewer's advice, this Figure caption was improved.

Revision:

Figure 3. Variations in MDA8 (Unit: μg/m³) of polluted cities from 2015 to 2018, including (a) Beijing **(capital of China)**, Tianjin and Tangshan **near the capital city**; (b) Taiyuan, Weifang and Shijiazhuang **in the south of NCH**; (c) Shanghai and Nanjing **in YRD**; and (d) Zhongshan and Guangzhou **in PRD**. The cities in panels (a)-(d) were located from north to south **and were illustrated in Figure S2**. The horizontal dash lines indicated the value of 100 μg/m³ and 215 μg/m³.

Figure 3: Add to Figure 3 caption what the dashed lines in panels b and d represent. I assume horizontal are the standard deviation and the vertical separate the years.

Reply:

According to the reviewer's advice, this Figure caption was improved.

Revision:

Figure 4. The first EOF pattern (PAT1: a, b) and second EOF pattern (PAT2: c, d) of MDA8 in summer from 2015 to 2018, including the spatial pattern (a, c) and the time coefficient (b, d). The black boxes in panels a and c are the selected North China and Huanghuai region (NCH), North China (NC), Yangtze River Delta (YRD) and Pearl River Delta (PRD). The EOF analysis were applied to the daily MDA8 anomalies at 868 stations to extract the relatively change features of the original data on the daily time-scale. The percentages on panel (b) and (d) were the variance contributions of the first and second EOF mode. **The horizontal dash lines indicated one standard deviation, and the vertical ones separated the years.**

Figure 5, 6, 10, 11: The units for water vapor flux are written as kg*m/(kg*s) which is a bit odd. I strongly encourage the authors to use negative values to indicate denominators in units throughout the paper. This would change these units to kg m kg-1 s-1 which then leads me to my next question whether these are the correct units. In its current form are the kg's representing different things (dry air vs

moisture?)

Reply:

We correct units as $gcm^{-1}s^{-1}hpa^{-1}$ which is widely adopted in research.

Revision:

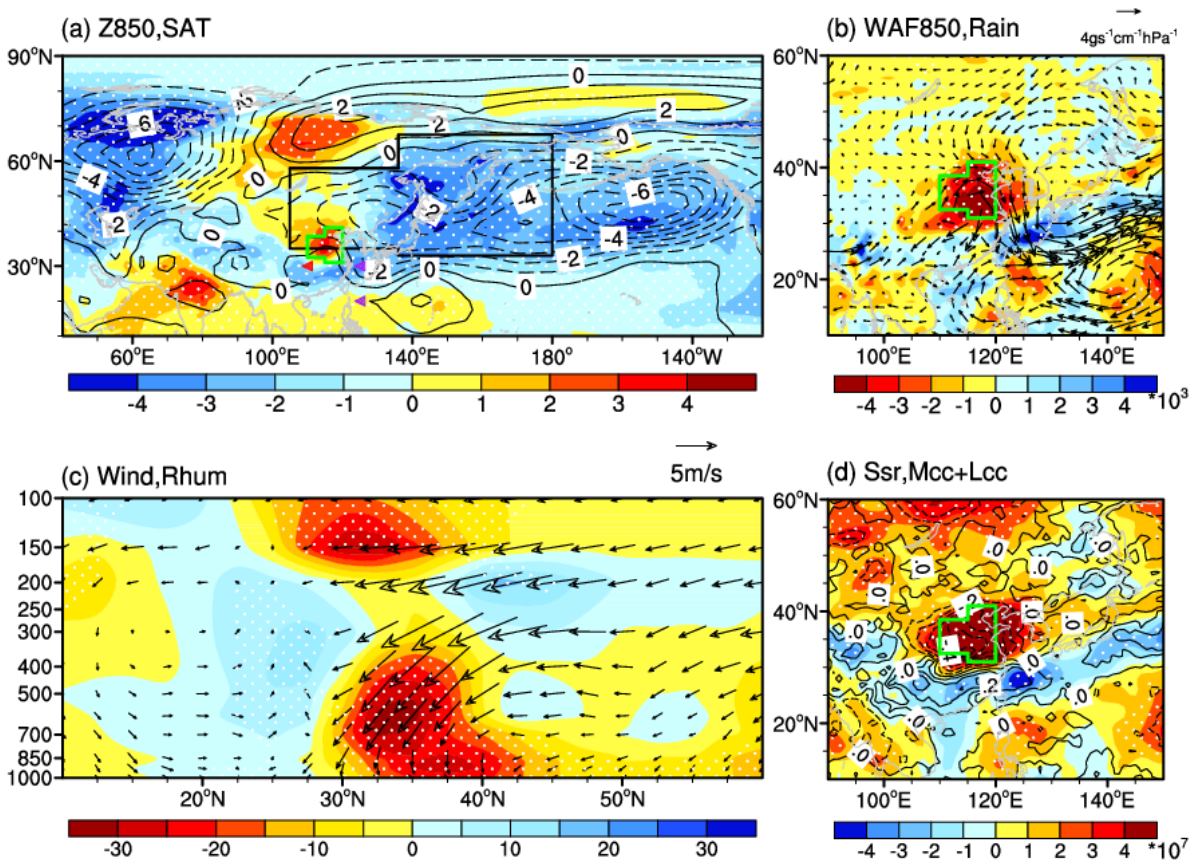

Figure 6. Differences of the daytime atmospheric circulations (i.e., PAT1P minus PAT1N). (a) Geopotential height at 850 hPa (Unit: 10gpm, contours) and surface air temperature (Unit: K, shading), (b) water vapor flux (Unit:$gs^{-1}cm^{-1}hpa^{-1}$) at 850 hPa (arrows) and precipitation (Unit: mm, shading), (c) 100°E–120°E mean wind (Unit: m/s, arrows) and relative humidity (Unit: %, shading), (d) downward solar radiation at the surface (Unit:10^7 J/m^2, shading) and the sum of low and medium cloud cover (Unit: 1, contours). The white dots indicate that the shading was above the 95% confidence level. The green boxes in panels (a), (b) and (d) show the NCH region, and the black box in panel (a) indicates the location of the East Asia trough. The purple triangles in panel (a) indicated the data used to calculate the $WPSH_1$, while the red triangle represented the west ridge point of WPSH.

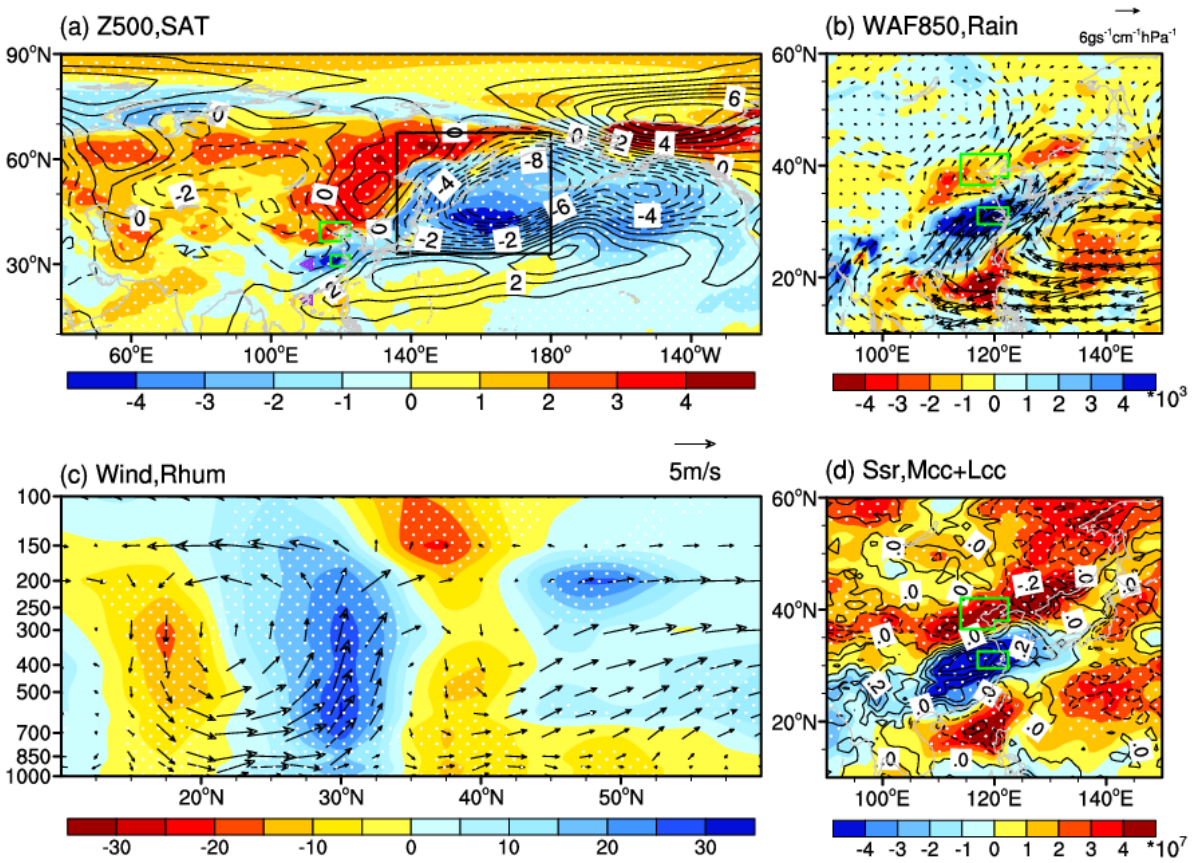

Figure 7. Differences of the daytime atmospheric circulations (i.e., PAT2P minus PAT2N). (a) Geopotential height at 500 hPa (Unit: 10gpm, contours) and surface air temperature (Unit: K, shading), (b) water vapor flux (Unit:$gs^{-1}cm^{-1}hpa^{-1}$) at 850 hPa (arrows) and precipitation (Unit: mm, shading), (c) 100°E–120°E mean wind (Unit: m/s, arrows) and relative humidity (Unit: %, shading), (d) downward solar radiation at the surface (Unit: $10^7 J/m^2$, shading) and the sum of low and medium cloud cover (Unit: 1, contours). The white dots indicate that the shading was above the 95% confidence level. The green boxes in panel (a), (b) and (d) are the NC and YRD regions, and the black box in panel (a) indicates the location of the East Asia trough. The purple triangles in panel (a) indicated the data used to calculate the $WPSH_2$.

Figure 7: It is difficult to see the crosses when the O3 anomaly is less than -25 ppb (the dark blue color). Can that be adjusted? Or maybe have white crosses instead? Also the y-axis minor tick marks are an odd spacing compared to the major 5 degree labelled tick marks. Can these minor tick marks be changed to maybe every 1 degree?

Reply:

According to the reviewer's advice, the Figure 5 was re-plotted. For example, the color bar was re-scaled and the label marks of y-axis was re-divided.

Revision:

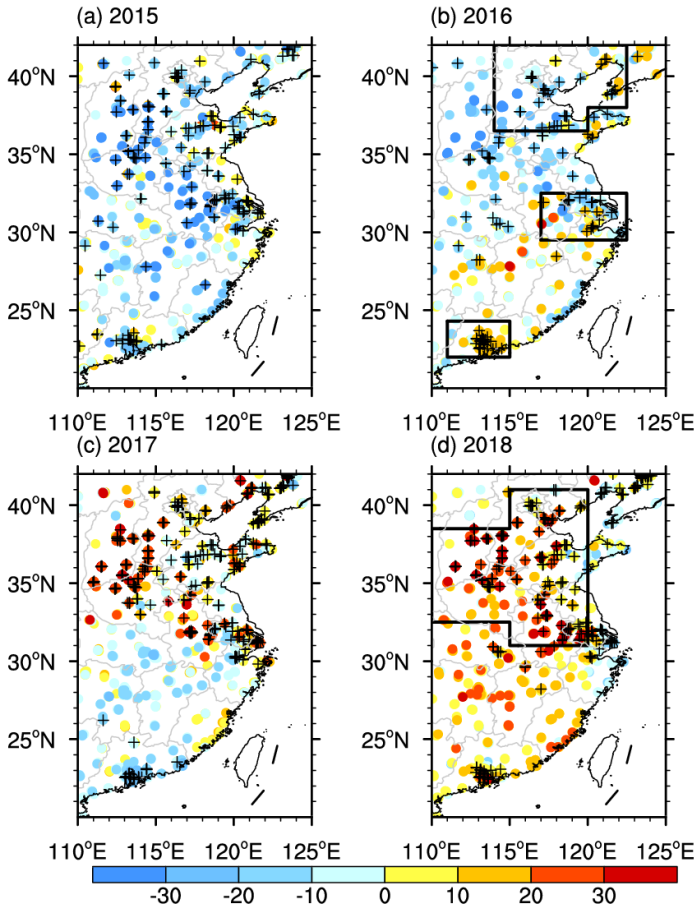

Figure 2. Anomalies of the summer mean MDA8 (Unit: μg/m³) in 2015 (a), 2016 (b), 2017 (c) and 2018 (d), relative to the mean during 2015–2018. The black pluses indicate that the maximum MDA8 was larger than 265 μg/m³.

Figure 9: Are the variations in reference to an average for all available sites in the NC and the YRD regions? If so, please add this level of detail to the Figure 9 caption.

Reply:

According to the reviewer's advice, this Figure caption was improved.

Revision:

Figure 9. Variations in the MDA8 (Unit: μg/m³) of NC (black) and the YRD (blue) in 2016 (a) and 2018 (b). **The MDA8 was calculated as an average for all available sites in the NC and the YRD regions.**

Response to Reviewer #2

The quality of the manuscript has been improved. The revised manuscript is much easier to follow, and the figures are carefully labeled and explained. Overall the authors have well addressed my concerns, but I'm confused with the authors' reply to my first comment regarding the impact of anthropogenic emissions.

In the first point, the authors clarify they are more interested in the fluctuation of MDA8 ozone, but the inter-annual variations in emissions should also have impacts on the anomalies of MDA8 ozone.

In the second point, the authors argue that the emissions are stable at daily scale and it's hard to acquire daily emission data, but I don't think this argument justifies why the impacts of emissions on the inter-annual variability of ozone (i.e. Figure 7) are not accounted. I'd suggest the authors provide some discussions on how the recent decreasing trends of NOx emissions could impact on the inter-annual variability of ozone.

Reply:

(1) As regards the mechanisms, our study mainly focus on the impacts of meteorological conditions on daily time-scale.

(2) The discussion of the impact of decreasing trends of NOx was really absent, which was strengthened in the revised manuscript and can be found in the following revisions.

(3) **According to the other reviewer's comment, we decided to delete the Figure 10 and 11, i.e., the iner-annual variability of ozone was not discussed in this revised version.** We now focus on the dominant patterns and their varying features in different years. Some new works will be supplemented and we will revisit the Figure 10 and Figure 11 in a later manuscript.

The contents related to Figure 7–9 were rewritten and redistributed in the revised version. The texts associated Figure 10 &11 were deleted. Detailed revisions can be found in the revised manuscript and also the mark-up manuscript.

Revision in the Introduction:

……Although deep stratospheric intrusions may elevate surface ozone levels (Lin et al., 2015), the main source of surface ozone is the photochemical reactions between the oxides of nitrogen (NO_x) and volatile organic compounds (VOC), i.e., NO_x + VOC = O_3. The concentrations of NO_x and VOC are fundamental drivers impacting ozone production, and are sensitive to the regime of ozone formation, i.e., NO_x-limited or VOC-limited (Jin and Holloway 2015)……

Revision in the first paragraph of Section 3:

……Surface O_3 pollution was closely linked to the anthropogenic emissions that dispersed and concentrated in the large cities (Fu et al., 2012), which was similar to the haze pollution (Yin et al., 2015). In the megacity cluster, the photochemical regime for ozone formation is combination of NO_x-limited and VOC-limited regimes (Jin and Holloway 2015). In the YRD and PRD, high levels of MDA8 were scattered around the large cities. Due to high emissions of NO_x both in large and small cities in the NCH region, the high-level O_3 values were contiguous, indicating extensively surface O_3 pollution (Figure 1)……

Revision in the Conclusions and Discussions:

……In this study, we mainly emphasized the contribution of the meteorological impacts and assumed the emissions of ozone precursors were relatively stable on the daily time-scale. Observational and modelling studies suggested that photochemical production of ozone in the NC, YRD and PRD was the transitional regime (i.e., both reductions of NO_x and VOC would reduce O_3), which would influence the concentrations of surface ozone (Jin and Holloway 2015). There is no doubt that the human activities were the fundamental driver of air pollution even on the daily time-scale, thus the joint effects of the daily meteorological conditions and anthropogenic emissions (including the photochemical regimes) needed to be discussed in future work……

Dominant Patterns of Summer Ozone Pollution in Eastern China and Associated Atmospheric Circulations

Zhicong Yin [12], Bufan Cao[1], Huijun Wang[12]

[1]Key Laboratory of Meteorological Disaster, Ministry of Education / Joint International Research Laboratory of Climate and Environment Change (ILCEC) / Collaborative Innovation Center on Forecast and Evaluation of Meteorological Disasters (CIC-FEMD), Nanjing University of Information Science & Technology, Nanjing 210044, China

[2]Nansen-Zhu International Research Centre, Institute of Atmospheric Physics, Chinese Academy of Sciences, Beijing, China

Correspondence to: Zhicong Yin (yinzhc@163.com)

Abstract. Surface ozone has been severe during summers in the eastern parts of China, damaging human's health and flora and fauna. During 2015–2018, ground-level ozone pollution increased and intensified from south to north. In North China and Huanghuai region, the O_3 concentrations were highest. Two dominant patterns of summer ozone pollution were determined, i.e., a south-north covariant pattern and a south-north differential pattern. The anomalous atmospheric circulations composited for the first pattern manifested as a zonally enhanced East Asia deep trough and as a west Pacific subtropical high whose western ridge point shifted northward. The local hot, dry air and intense solar radiation enhanced the photochemical reactions to elevate the O_3 pollution levels in North China and Huanghuai region, however the removal of pollutants were decreased. For the second pattern, the broad positive geopotential height anomalies at high latitudes significantly weakened cold air advection from the north, and those extending to North China resulted in locally high temperature near the surface. In a different manner, the west Pacific subtropical high transported sufficient water vapor to the Yangtze River Delta and resulted in locally adverse environment for the formation of surface ozone. In addition, the most dominant pattern in 2017 and 2018 was different from that in previous years, which is investigated as a new feature. ~~Furthermore, the implications for the interannual differences in summer O_3 pollution have also proven to be meaningful.~~

1. Introduction

High levels of ~~O~~ozone occurs both in the stratosphere and at the ground level. Stratospheric ozone forms a protective layer that shields us from the sun's harmful ultraviolet radiation. However, surface ozone is an air pollutant and has harmful effects on people and on the environment, such as damaging human lungs (Day et al., 2017) and destroying agricultural crops and forest vegetation (Yue et al., 2017). Worldwide, ~~severe~~ polluted ozone events are more frequent and stronger in China than those that have taken place in Japan, South Korea, Europe, and the United States (Lu et al., 2018). Due to their close relationship with anthropogenic emissions (Li et al., 2018), the high O_3 concentrations in China are mainly observed in urban regions, such as in North China (NC, ~~114 °E–122.5 °E, 36.5 °N–42 °N~~Figure 1b), the Yangtze River Delta (YRD~~, 117 °E–122.5 °E, 29.5 °N–32.5 °N~~) and the Pearl River Delta (PRD~~, 111 °E–115 °E, 22 °N–24.3 °N~~) where rapid development has

occurred in recent decades (Wang et al., 2017). An increase in surface ozone levels was found in China in 2016 and 2017 relative to 2013 and 2014 (Lu et al., 2018). The O_3 pollution levels in Beijing-Tianjin-Hebei (part of NC) were the most severe in China (Wang et al., 2006; Shi et al., 2015) and this situation has been getting worse. The O_3 concentrations in North China underwent a significant increase in the period of 2005–2015, with an average rate of 1.13 ±0.01 ppbv yr^{-1} (Ma et al., 2016). Although far away from the anthropogenic emissions, ~~Even on the highest mountain over NC, Mount Tai,~~ the summer (June-July-August, JJA) O_3 on the highest mountain over NC (Mount Tai) increased significantly by 2.1 ppbv yr^{-1} from 2003 to 2015 (Sun et al., 2016). The O_3 levels generally presented increasing trends from 2012 to 2015 in the YRD (Tong et al., 2017), e.g., the O_3 concentrations in Shanghai (a mega-city) increased by 67% from 2006 to 2015 (Gao et al., 2017). In the PRD region, O_3 increased by 0.86 ppbv yr^{-1} from 2006 to 2011 (Li et al., 2014). Furthermore, ~~Severe o~~ozone pollution is projected to increase in the future over eastern China (Wang et al., 2013).

Although deep stratospheric intrusions may elevate surface ozone levels (Lin et al., 2015), the main source of surface ozone is the photochemical reactions between the oxides of nitrogen (NO_x) and volatile organic compounds (VOC), i.e., NO_x + VOC = O_3. The concentrations of NO_x and VOC are fundamental drivers impacting ozone production, and are sensitive to the regime of ozone formation, i.e., NO_x-limited or VOC-limited (Jin and Holloway 2015). The changes in fine particulate matter are also a pervasive factor for the variation in ozone concentration. Employed the ~~Goddard Earth Observing System~~GEOS-Chem ~~Chemical~~ chemical ~~Transport~~ transport ~~Model~~model, Li et al. (2018) found that rapid decreases in fine particulate matter levels significantly stimulated ozone production in NC by slowing down the aerosol sink of hydro-peroxy radicals. ~~Furthermore~~In addition, the meteorological conditions also influenced the ozone levels via modulation of the photochemical episodes and removal effects (Yin et al., 2019; Lu et al., 2019). Intense solar radiation accelerated chemical O_3 production (Tong et al., 2017). A severe heat wave in the YRD contributed to high O_3 concentrations in 2013 (Pu et al., 2017). Winds had an impact on the O_3 and its precursors at downwind locations (Doherty et al., 2013). Local meteorological influences are always related to specific large-scale atmospheric circulations. The changes in the East Asian summer monsoon led to 2–5% interannual variations in surface O_3 concentrations over central eastern China (Yang et al., 2014). Continental anticyclones created sunny and calm weather, which are favourable conditions for O_3 production in NC (Ding et al., 2013; Yin et al., 2019). Due to the associated transports of pollution from inland, tropical cyclones are often related to the evaluation of surface O_3 levels in the coastal areas of PRD (Ding et al., 2004). Basing on a case study in 2014, further studies showed that a strong west Pacific subtropical high (WPSH) was unfavourable for the formation of O_3 in South China (Zhao and Wang, 2017), however the physical mechanisms to impact O_3 in North China was still not sufficiently explained. Thus, in addition to human activities and secondary aerosol processes, the impacts of atmospheric circulations and meteorological conditions must be systematically studied to improve understanding of the O_3 pollution in North China.

~~Wang et al. (2017) reviewed the meteorological influences on ozone events, but the referenced findings were published~~

~~mainly before 2010, when measurements in China were still scarce.~~ Since 2015, O_3 measurements in eastern China were steadily and widely implemented, but the O_3-weather studies mainly focused on meteorological elements (e.g. temperature, precipitation etc.) and several synoptic processes (Xu et al., 2017; Xiao et al., 201~~3~~7). The dominant patterns of daily ozone in summer in east of China are still unclear. In this study, we built upon the previous literatures analysing ozone and meteorological influences thanks to the availability of more ozone observations by the Chinese government since 2015, providing us more information to analyse than available in these earlier studies, e.g., Zhao and Wang (2017)~~Actually, in our study, we found the most dominant pattern was different with that in Zhao and Wang (2017) and the dominant patterns also showed interannual variations~~. The findings of this study basically help to understand the varying features of daily surface ozone pollution in eastern China and~~,~~ their relationships with large-scale atmospheric circulations ~~and the implications for the climate variability~~.

2. Data sets and methods

Nationwide hourly O_3 concentration data since May 2014 are publicly available on http://beijingair.sinaapp.com/. Since the severe air pollution events in 2013, the air pollution issues gained more attentions from the Chinese government and society, which aided to start the extensive constructions of operational monitoring stations of atmospheric components and resulted in continuous increasing number of sites (Figure S1). The number of sites in eastern China (110°E–125°E, 22°N–42°N) was 677, 937, 937, 995 and 1007 from 2014 to 2018. It is obvious that the data in 2014 were deficient, while the observations were broadly distributed in eastern China and continuously achieved since 2015. Thus, the summer O_3 data from 2015 to 2018 were processed (e.g., unifying the sites and eliminating the missing value) and 868 sites in eastern China were employed here to reveal some new features of surface ozone pollutions and associated anomalous atmospheric circulations. Generally, severe air pollutions occurred more frequently in cites than in rural areas, therefore, the monitoring sites of atmospheric components mostly gathered around the urban areas, indicating the results of this study were more suitable ~~to~~ for the urban O_3 pollution. The maximum daily average 8 h concentration of ozone (MDA8) is the maximum of the running 8 h mean O_3 concentration during an entire 24 hour day. According to the Technical Regulation on Ambient Air Quality Index of China (the Ministry of Environmental Protection of China, 2012), MDA8 is generally used to represent the daily O_3 conditions. The MDA8 $\in$ [0, 100], (100, 160], (160, 215], (215, 265], (265, 800] μg/m³ corresponds to “Excellent”, “Good”, “Lightly polluted”, “Moderately polluted”, “Heavily polluted” levels of air quality in China.

The 2.5 °×2.5 °ERA-Interim data used here include the geopotential height (Z) at 850 and 500 hPa, zonal and meridional wind, relative humidity, vertical velocity, air temperature ~~at~~ from surface to 100 hPa, surface air temperature (SAT) and wind, downward solar radiation at the surface, low and medium cloud cover and precipitation (Dee et al., 2011). Because the maximum photochemical activity often occurred at afternoon (Wang et al., 2010), the daytime data were calculated by the

6-hourly reanalysis (including Z, wind, relative humidity, vertical velocity, air temperature and cloud cover) and 3-hourly ~~reanalysis~~ data (precipitation and downward solar radiation) to composite the daytime atmospheric circulations and daytime meteorological conditions. Due to the different representative period of each element in ERA-Interim data, the daytime for Z, wind, relative humidity, vertical velocity, air temperature and cloud cover was from 05 ~~a.m.~~ to ~~05 p.m~~17 (Beijing Time; 21 ~~p.m.~~ 09 ~~a. m.~~ UTC), while it is from 08 ~~a.m.~~ to ~~08 p.m.~~20 (Beijing Time; 00 ~~a.m.~~ to ~~00 p.m.~~12 UTC) for precipitation and downward solar radiation.

The empirical orthogonal function (EOF) analysis is a widely used statistical method in meteorology to reconstruct the original variables into several irrelevant patterns (Wilks, 2011). The EOF analysis, applied to the daily anomalies (MDA8 anomalies at 868 stations in this study), extracted the relative~~ly~~ change features of the original data on the daily time-scale. The orthogonal modes included spatial and temporal coefficients, and contained information of some proportion (variance contributions) from the original fields. Significance test must be execute to confirm whether the decomposed patterns had physical meanings. In this study, we used the test method form North et al.~~,~~ (1982). That is, if the eigenvalue (λ) satisfied the condition as $\lambda_i - \lambda_{i+1} \geq \lambda_i(2/n)^{1/2}$, the eigenvalue λ_i was significantly separated. We performed this significance test on the selected patterns from EOF decompositions, and confirmed that these dominant patterns in this study were all significant. The aforementioned EOF analysis programs were finished by the NCAR Command Language.

3. Variations and dominant patterns

During 2015–2018, summer surface ozone pollution was severe in China, especially in the economically developed regions. Spatially, the JJA mean MDA8 increased from south to north in eastern China (Figure 1a). To the south of 28°N (i.e., South China), the mean MDA8 was mostly lower than 100 μg/m³ and ~~the ozone pollution was obviously~~ lower than ~~that~~ the O_3 pollution in North China and in the Huanghuai area (NCH, Figure 1a). It is notable that, although the values of MDA8 in the PRD were not as large as those in NCH, they were relatively higher than those in the surrounding areas. The mean MDA8 was above 110 μg/m³ to the north of 32°N (i.e., the NCH area), and thereinto, the large values of MDA8 centred on the Beijing-Tianjin-Hebei region and in western Shandong province exceeded 150 μg/m³. In the transitional zone, i.e., between 28°N and 32°N, the MDA8 varied from 100 μg/m³ to 120 μg/m³. Surface O_3 pollution was closely linked to the anthropogenic emissions that dispersed and concentrated in the large cities (Fu et al., 2012), which was similar to the haze pollution (Yin et al., 2015). In the megacity cluster, the photochemical regime for ozone formation is combination of NO_x-limited and VOC-limited regimes (Jin and Holloway 2015). In the YRD and PRD, high levels of MDA8 were scattered around the large cities. ~~However,~~ Due to high emissions of NO_x both in large and small cities in the NCH region, the high-level O_3 values ~~in the NCH region~~ were contiguous, indicating extensively ~~severe~~ surface O_3 pollution ~~both in large and small cities~~ (Figure 1). Furthermore, the maximum values of MDA8 for four summers were extracted to evaluate the severest levels of O_3 pollution (Figure 1b). To the

north of 30°N, the maximum MDA8 at most sites was above 265μg/m³ (i.e., the threshold of heavily O_3 pollution in China), indicating that ~~the levels of~~ heavily O_3 pollution had occurred. ~~exceeded the threshold of heavily O_3 pollution in China (The Ministry of Environmental Protection of China, 2012).~~ The observed summer MDA8 anomalies in eastern China also presented evident interannual differences (Figure 2). The number of sites with maximum MDA8 > 265 μg/m³ in NCH (YRD) was 94 (35), 55 (22), 180 (58), 160 (46) from 2015 to 2018 (Figure 2). The summer mean MDA8 in the PRD was not as high as that in NC and the YRD (Figure 1a), but maximum O_3 concentration exceeded 265 μg/m³ could also be observed in certain large cities of PRD in each year (Figure 2).

Ten cities, with ~~severe~~ O_3 pollutions, were chosen to investigate the temporal variations, including Beijing (capital of China), Tangshan, Tianjin near the capital city, Shijiazhuang, Weifang and Taiyuan in the south of NCH, Nanjing and Shanghai in YRD, Guangdong and Zhongshan in PRD (Figure S2). These cities had large populations and were with ~~severe~~ high levels of O_3 pollutions. In Beijing, Tianjin and Tangshan, the MDA8 values were nearly above 100 μg/m³ and frequently exceeded 215 μg/m³ (Figure ~~2~~3a). The percentage of non-O_3-polluted days (<100 μg/m³) and moderate O_3-polluted days (>215 μg/m³) were 14.9% and 15.5% for the mean MDA8 of these three cities. The former percentage indicated that more than 85% O_3 concentrations exceeded the health threshold (i.e., the upper limit "Excellent" level), and the later meant, in more than 15% of summer days, O_3 concentrations moderately damaged human health in the Beijing-Tianjin-Hebei region. The maximum MDA8 in the north of Hebei province (e.g. Tangshan in Figure ~~2~~3a) and in eastern Shandong province (e.g. Weifang in Figure ~~2~~3b) even exceeded 320 μg/m³, which badly injured the health of local citizens. In Shijiazhuang, Weifang and Taiyuan, the MDA8 levels were lower than those in Beijing and Tianjin during 2015–2016, but dramatically increased to levels comparable to those of Beijing and Tianjin in 2017 and 2018 (Figure ~~2~~3a, b). In Nanjing and Shanghai, the MDA8 did not show a clear increasing trend (Figure ~~2~~3c). Similar to the distribution of the mean MDA8, the maximum MDA8 to the south of 30°N was lower by comparison. Although approximately 60% of summer days were non-O_3-polluted in the cities of Guangzhou and Zhongshan (Figure ~~2~~3d), heavily polluted ~~severe~~ O_3 pollution also occurred in the PRD (Figure 1b).

Considering the characteristics of the observed MDA8 mentioned above, EOF approach was used to explore the dominant patterns of summer ozone pollution in eastern China (Figure ~~3~~4). The percentages of variance contribution for the first three patterns were 21.5%, 15.5% and 8%. The significance test of the EOF eigenvalues confirmed that the first three patterns were significantly separated. Approximately 37% of the variability in the original data was contained in the first two patterns, therefore, they were defined as the dominant patterns of surface ozone pollution on the daily time-scale. In the first EOF pattern (PAT1), the observed MDA8 at different sites changed similarly and the centre of variation was located in the NCH area (Figure ~~3~~4a). The time series of EOF1 showed that the ozone pollution during 2017–2018 was more serious than that in 2015 and 2016 (Figure ~~3~~4b). Differently, the second EOF pattern (PAT2), showed notable south-north difference, with centres in the

NC and YRD regions (Figure ~~3~~4c). The time coefficient of PAT2 ~~also~~ did not show an obvious increasing trend (Figure ~~3~~4d). The positive (P) and negative (N) phases of PAT1 (PAT1P, PAT1N) and PAT2 (PAT2P, PAT2N) are defined by the events that are greater than one standard deviation and less than ~~-~~1 ×one standard deviation, respectively (Figure ~~3~~4b, ~~3~~4d).

Figure ~~3~~4 illustrates the EOF results for the dominant patterns of surface ozone, while Figure ~~4~~5 show~~ed~~ the MDA8 composites break down into the positive and negative phases. The ozone concentrations for the PAT1P classification (Figure ~~4~~5a) were generally greater than those for PAT1N (Figure ~~4~~5b). Most of the MDA8 values in the NCH region were >160 μg/m³ and <120 μg/m³ for PAT1P and PAT1N, respectively (Figure 5a, b). For the second pattern, the PAT2P appeared as a diminishing pattern from the north to the south (Figure ~~4~~5c), however, there was ~~severe~~ high concentrations of ozone pollution in the YRD and PRD under PAT2N conditions (Figure ~~4~~5d). Therefore, the centres of O_3 variation were NCH for the PAT1, and NC and the YRD for the PAT2.

4. Associated atmospheric circulations

In eastern China, despite the economic productions and human actives steadily ~~developed~~ increased in the ~~recent~~ four years of study and we assume the emissions of ozone precursors to be ~~were reasonably supposed to be~~ relatively stable on the daily time-scale. Differently, the daily variations in MDA8 were evidently saw in Figure ~~2~~3. Therefore, the impacts of daily meteorological conditions significantly contributed to the domain patterns of daily O_3 concentrations and their variations. Anomalous daytime atmospheric circulations associated with PAT1 (PAT1P composite minus PAT1N composite) and PAT2 (PAT2P composite minus PAT2N composite) ~~were~~ are shown Figure ~~5~~6 ~~6~~7. ~~For example, the mean of the atmospheric circulations associated PAT1P (PAT1N) were firstly computed, and then the differences between PAT1P composites and PAT1N composites were calculated as the anomalous daytime atmospheric circulations associated with PAT1.~~ For the first pattern, the largest O_3 differences between the PAT1P and PAT1N was within the NCH region (Figure ~~4~~5a, b). The correlation coefficient between the time series of PAT1 and the NCH-averaged MDA8 was 0.97 (Table 1). Thus, the effects of the anomalous atmospheric circulations mainly acted on the photochemical reactions near the surface in NCH and the removal of pollutants. In Figure 6a, ~~T~~there were negative Z850 anomalies over the Ural Mountains. Over the broad region from eastern Eurasia to the north Pacific, the anomalous atmospheric circulations were located zonally, i.e., positive Z850 on the tropical zone, cyclonic anomalies at the mid to high latitudes and positive anomalies on the polar region (Figure ~~5~~6a). The East Asia deep trough was enhanced and extended to northeast China and Japan. The intensity of the East Asia deep trough (i.e., the negative area-averaged Z850) positively correlated with the time series of PAT1 (EAT, Table 1) with a correlation coefficient of 0.28 (above the 99% confidence level). In accordance with the deep positive height anomalies to the north of Lake Baikal (centring at 107 °E, 53.5 °N), which also extended southward to the edge of the Tibetan Plateau (Figure 6a), cold air was transported to the lower latitudes. However, local anti-cyclonic circulation over NCH prevented the cold air to ~~but did not~~

arrive at the NCH region (Figure ~~5~~6~~a~~b).

Influenced by the enhanced East Asia deep trough, the main body of WPSH shifted southward (compared to its climate status in summer). The location of WPSH ($Z500_{(125^0E,\ 20^0N)} - Z500_{(125^0E,\ 30^0N)}$) also showed a positive correlation with the time series of PAT1 (R=0.39, Table 1). However, the western ridge point of WPSH was northward and westward than normal (being indicated by$Z500_{(110^0E,\ 30^0N)}$), and occupied the NCH area, which was significant with the time series of PAT1 (R=0.24, above the 99% confidence level). Although the local anomalous anticyclone over the east of China seemingly delivered water vapor to North China (Figure ~~5~~6b), the channel of moisture was already cut off in the ocean at low latitudes by the positive and zonal anomalies in the tropical regions (Figure ~~5~~6a) and resulted in a dry environment in NCH from surface to 400 hPa (Figure ~~5~~6c). Furthermore, the associated descending motions (Figure ~~5~~6c) not only corresponded to the warmer surface air temperature (Figure ~~5~~6a), but also suppressed the development of convective activity (indicating by less low and medium cloud, Figure ~~5~~6d). The correlation coefficients between the time series of PAT1 and NCH-averaged precipitation, SAT, and downward solar radiation at surface were –0.44, 0.14 and 0.45, respectively, all of which exceeded the 99% significance test (Table 1). The large-scale atmospheric circulations led to days with high temperatures near the surface (Figure ~~5~~6a), less precipitation (Figure ~~5~~6b), a dry environment (Figure ~~5~~6c) and intense solar radiation (Figure ~~5~~6d), which substantially enhanced the generation of ozone in NCH but weakened the removal of the pollutants.

For PAT2, largest O_3 differences (PAT2P composite minus PAT2N composite) were observed in the NC and YRD regions (Figure ~~3~~4c, Figure ~~4~~5c, d). The correlation coefficient between the time series of PAT2 and the MDA8 difference between NC and the YRD was 0.77 (Table 1). The impacts of atmospheric circulations on the photochemical reactions and removal effects in the above two areas are analysed in Figure ~~6~~7. It is notable that the signals of atmospheric circulations were clearer at the lower troposphere (i.e., 850 hPa) for PAT1 (Figure 6a), however, the signals for PAT2 could be recognized both at the low- and mid- troposphere (Figure 7a). Due to the broad positive Z500 anomalies at the high latitudes of Eurasia, the subjacent surface air temperatures significantly increased, indicating weak cold air advection from the north (Figure ~~6~~7a). Moreover, there were positive Z500 anomalies from the Chukchi Peninsula (about cantering at 180 °E, 66.5 °N) to Northeast China. In summer, anomalous anticyclonic circulations at the mid and high latitudes generally led to significantly positive SAT anomalies (Figure ~~6~~7a). The East Asia deep trough was stronger (R=0.3), but was limited to the ~~east~~ Sea of Japan.

Extruded by the East Asia deep trough and cyclonic anomalies from the Siberian plains to the YRD, the WPSH moved southward and exhibited southwest-northeast orientation (Figure ~~6~~7a). The location of WPSH ($Z500_{(110^0E,\ 20^0N)} - Z500_{(110^0E,\ 30^0N)}$) was positively correlated with the time series of PAT2 (R=0.32, Table 1). The southwest-northeast distribution of WPSH aided water vapor transportation to the YRD region (Figure ~~6~~7b–c). Combined with significant upward air flow (Figure ~~6~~7c), more clouds formed at the medium and low levels (Figure ~~6~~7d) and precipitation was enhanced in the YRD region (Figure ~~6~~7b). A moist-cool environment, weak solar radiation and ~~obvious~~ wet deposition reduced the ozone

concentration in the YRD region. On the other hand, sinking motion (Figure ~~6~~7c) and less cold air advection from the north (Figure ~~6~~7a) both resulted in a temperature increase in NC (Figure ~~6~~7a). There was divergence of water vapor and less cloud cover over NC, resulting in dry, hot and sunny weather (Figure ~~6~~7b, d). Under such meteorological conditions, the generation of surface O_3 was accelerated but the removal processes were slowed down, and thus, higher MDA8 was observed in NC. The differences in precipitation, SAT, and downward solar radiation at the surface between the NC and YRD regions were calculated and their correlation coefficients with the time series of PAT2 were –0.46, 0.18 and 0.62, respectively (Table 1). The significant correlations indicated that the differences in meteorological conditions between NC and YRD regions, associated with the aforementioned anomalous atmospheric circulations, largely contributed to O_3 PAT2.

~~5. Signals for interannual variability~~

~~Additionally, the observed summer MDA8 anomalies in eastern China presented evident interannual differences (Figure 7). The dominant spatial patterns of MDA8 anomalies in each year were also different (Figure 8). Although the relative variance contributions of the spatial coefficients varied, the first two EOF patterns of MDA8 were always PAT1 and PAT2 in different years, indicating that the extracted dominant patterns were reliable and steady. Sorting by the variance contribution, the dominant patterns were PAT2 and PAT1 in 2015 and 2016 (Figure 8a–d), however, they are PAT1 and PAT2 in the two subsequent years (Figure 8e–h). The first EOF pattern in 2014 revealed by Zhao and Wang (2017) was similar with PAT2, however the most dominant pattern changed to PAT1 in the latest two years (2017 and 2018).~~

~~A question raised here is whether the aforementioned composited signals of atmospheric circulations could provide implications for the climate variability of the summer O_3 pollution in eastern China. In 2016 and 2018, the variance contribution of the first pattern was almost twice that of the second pattern, and thus, these two years were selected as typical years whose varied patterns were clearly separated. The dominant pattern of 2016 was PAT2 (explaining approximately 24% of the variance, Figure 8e), while that in 2018 changed as PAT1, with nearly 34% variance contributions (Figure 8g). In 2016, the MDA8 values in NC and the YRD were nearly out of phase (Figure 9a), and the correlation coefficient between them was –0.28 (above the 99% confidence level). Differently, this correlation coefficient was 0.43 in 2018 (Figure 9b), indicating similar change features between the MDA8 levels of NC and the YRD.~~

~~The MDA8 anomalies in 2016 were negative in NC, but positive in the YRD and PRD (Figure 7b), which was the opposite pattern of PAT2. The interannual anomalies of atmospheric circulations in 2016, with respect to the mean of 2015–2018 (Figure 10), were almost opposite to the anomalous atmospheric circulations associated with PAT2 (Figure 6). There were positive Z500 anomalies over the north Pacific at the mid to high latitudes (Figure 10a). These positive anomalies not only indicated a weaker East Asia deep trough but also induced a shallow trough from the Chukchi Peninsula to Northeast China. Together with the stronger high ridge over the Ural Mountains, the cold air was transported to the mid latitudes,~~

~~resulting in a lower SAT in North China (Figure 10a). The western segment of the WPSH was stronger and moved northward, which occupied the YRD and south China (Figure 10a) and brought moist air flows to North China (Figure 10b). Sufficient moisture formed more low to mid-level clouds, causing a decrease in solar radiation reaching the ground in NC (Figure 10d). Associated with the extending WPSH, sinking motions resulted in a hot, dry air mass near the surface in the YRD region (Figure 10b–c). In addition, decreased cloud cover did not effectively reflect solar radiation, which was an essential condition for the enhancement of the photochemical reactions. Therefore, at the interannual time scale, the atmospheric anomalies, opposite to those shown in Figure 6, also played important roles on the spatial pattern of MDA8 anomalies. That is, the atmospheric circulations in 2016 accelerated the formation of surface O_3 in the south of YRD, but weakened the summer O_3 pollution in NC.~~

~~The MDA8 anomalies were mostly positive in the east of China in 2018 (Figure 7d). " + " pattern of Z850 anomalies were located over the Ural Mountains and to the north of Lake Baikal and the Aleutian Islands (Figure 11a), which was consistent with the anomalous patterns in Figure 5. The East Asia deep trough shifted northward than the mean status during 2015–2018, and meanwhile, the western ridge point of WPSH also shifted northward, resulting in a higher SAT in the east of China (Figure 11a) and accelerating the photochemical conversion for elevating the surface ozone concentration. The local anomalous anti-cyclone over the NCH and the Japan Sea also existed in the interannual signals, which induced the divergence of water vapor in southeast China (Figure 11b). Due to the lack of moisture, it was difficult to form cloud cover, and more solar radiation directly reached the ground (Figure 11d). The large-scale atmospheric circulations led to high temperatures near the surface in eastern China, and to a dry and sunny environment in the YRD and South China. Thus, under such weather conditions, positive MDA8 anomalies were observed in 2018. Although the signals of global warming had impacts on the anomalies of atmospheric circulations, the key features could also be found when the anomalies were viewed with respect to the climate mean during 1979–2018 (Figure S3–S4). In addition, if the variance contributions of the first two EOF patterns were not significantly different, i.e., in 2015 and 2017, the interannual signals of atmospheric circulations also showed integrated characteristics of PAT1 and PAT2 (Figure S5–S6).~~

~~8.~~5. Conclusions and discussions

At present, the fine particulate matter decreased in the summers in eastern China, and ~~During the recent four years,~~ ground-level ozone pollution became the major air challenge in the summers in the east of China (Li et al., 2018). The highest O_3 concentrations were observed in North China and in the Huanghuai region, which are located north of 32°N. The O_3-contaminated air occurred for 85% of summer days in Beijing and Tianjin. In the south, the surface O_3 pollution was also severe both in the Yangtze and Pearl River delta regions. Meteorological conditions had significant impacts on the evident daily fluctuation of MDA8. To reveal their detailed relationships, the dominant patterns of summer ozone pollution and

associated atmospheric circulations were analysed in this study.

The MDA8 of the first prominent pattern changed synergistically in the east of China, especially in North China and ~~in the~~ Huanghuai region. An enhanced East Asia deep trough and west Pacific subtropical high were zonally distributed and prevented the northward transportation of moisture. The northward-shifted western ridge point of the west Pacific subtropical high accelerated the photochemical reactions via hot-dry air and intense solar radiation, but weaken the removal of pollutants ~~via hot-dry air and intense solar radiation~~. The second pattern of ozone pollution showed remarkable south-north differences. Broad positive geopotential height anomalies at the high latitudes significantly decreased cold air advection from the north and thus increased the surface air ~~temperature~~ temperature~~and thus decreased cold air advection from the north~~. These positive anomalies also extended to North China and resulted in locally warmer air near the surface. On the other hand, the southwest-northeast oriented west Pacific subtropical high transported sufficient water vapor to the Yangtze River Delta. Consequently, a local moist-cool environment, without intense sunlight, reduced the formation of surface ozone.

~~Additionally, the observed summer MDA8 anomalies in eastern China presented evident interannual differences (Figure 7).~~ In addition to evident interannual differences of MDA8 anomalies (Figure 2), ~~T~~the dominant spatial patterns of MDA8 anomalies in each year were also different (Figure 8). Although the relative variance contributions of the spatial coefficients varied, the first two EOF patterns of MDA8 were always PAT1 and PAT2 in different years, indicating that the extracted dominant patterns were reliable and steady. Sorting by the variance contribution, the dominant patterns were PAT2 and PAT1 in 2015 and 2016 (Figure 8a–d), however, they are PAT1 and PAT2 in the two subsequent years (Figure 8e–h). The first EOF pattern in 2014 revealed by Zhao and Wang (2017) was similar with PAT2, however the most dominant pattern changed to PAT1 in the latest two years (2017 and 2018).

~~A question raised here is whether the aforementioned composited signals of atmospheric circulations could provide implications for the climate variability of the summer O_3 pollution in eastern China.~~ In 2016 and 2018, the variance contribution of the first pattern was almost twice that of the second pattern~~, and thus, these two years were selected as typical years whose varied patterns were clearly separated.~~. The dominant pattern of 2016 was PAT2 (explaining approximately 24% of the variance, Figure 8c), while that in 2018 changed as PAT1, with nearly 34% variance contributions (Figure 8g). In 2016, the MDA8 values in NC and the YRD were nearly out of phase (Figure 9a), and the correlation coefficient between them was –0.28 (above the 99% confidence level). Differently, this correlation coefficient was 0.43 in 2018 (Figure 9b), indicating similar change features between the MDA8 levels of NC and the YRD. The dominant patterns of ozone concentrations were decomposed with the observed data from 2015 to 2018. With the increase in O_3 observations, increasingly reliable dominant patterns and the reasons for the variation in dominant patterns might be revealed in the future.

In this study, we mainly emphasized the contribution of the meteorological impacts and assumed the emissions of ozone

precursors were relatively stable on the daily time-scale. Observational and modelling studies suggested that photochemical production of ozone in the NC, YRD and PRD was the transitional regime (i.e., both reductions of NO_x and VOC would reduce O_3), which would influence the concentrations of surface ozone (Jin and Holloway 2015). There is no doubt that the human activities were the fundamental driver of air pollution even on the daily time-scale~~. However, the daily emission data were difficult to be acquired~~, thus the joint effects of the daily meteorological conditions and anthropogenic emissions (including the photochemical regimes) needed to be discussed in future work. ~~The interannual differences in summer O_3 pollution were also discussed and the composited signals of atmospheric circulations and weather conditions proved to have meaningful implications for climate variability.~~ Lu et al.~~,~~ (2019) found that the observed 2017 surface ozone increases relative to 2016 in China are largely due to hotter and drier weather conditions, while changes in domestic anthropogenic emissions alone would have led to ozone decreases in 2017 basing on their GEOS-Chem experiments. ~~Although t~~The simultaneous large-scale atmospheric circulations ~~were diagnosed~~ on an interannual scale and~~,~~ their possible preceding climate drivers, e.g., sea ice, and sea surface temperature, were still unclear so far. The research related to climate variability has always needed long-term data. To get around the problem of the data time span, Yin et al. (2019) developed an ozone weather index using data from 1979 to 2017 and demonstrated the contributions of Arctic sea ice in May to O_3 pollution in North China. ~~In addition, the dominant patterns of ozone concentrations were also decomposed with the observed data from 2015 to 2018. With the increase in O_3 observations, increasingly reliable dominant patterns and more features might be revealed in the future. At present, the fine particulate matter decreased in the summers in eastern China (Li et al. 2018); however ozone production was significantly enhanced. Thus, attentions to surface pollution should be strengthened and the weather-climate component should be taken into account when making decisions for control measures.~~ According to the results, attentions to surface pollution should be strengthened and the weather-climate component should be taken into account when making decisions for control measures.

Data availability.

Hourly O_3 concentration data is supported by the website: http://beijingair.sinaapp.com (Ministry of Environmental Protection of China, 2018). Atmospheric circulation datasets are downloaded from http://www.ecmwf.int/en/research/climate-reanalysis/era-interim (ERA-Interim, 2018).

Author contribution.

ZY and HW designed the research. BC and ZY performed most of the Figures and analysis. ZY prepared the paper with

contributions from all co-authors.

Competing interests.

The authors declare that they have no conflict of interest.

Acknowledgements.

This research was supported by the National Natural Science Foundation of China (41421004, 91744311 and 41705058) and the funding of the Jiangsu Innovation & Entrepreneurship team.

References

Day, D. B., Xiang, J. B., Mo, J. H., Li, F., Chung, M., Gong, J. C., Weschler, C. J., Ohman-Strickland, P. A., Sundell, J., Weng, W. G., Zhang, Y. P., and Zhang J.: Association of Ozone Exposure ~~With~~ with Cardiorespiratory Pathophysiologic Mechanisms in Healthy Adults. JAMA Internal Medicine, 177(9), 1344-1353, doi:10.1001/jamainternmed.2017.2842, 2017.

Dee, D. P., Uppala, S. M., Simmons, A. J., Berrisford, P., Poli, P., Kobayashi, S., Andrae, U., Balmaseda, M. A., Balsamo, G., Bauer, P., Bechtold, P., and Beljaars, A. C. M.: The ERAInterim reanalysis: configuration and performance of the data assimilation system, Quarterly Journal of the Royal Meteorological Society, 137, 553–597, doi:10.1002/qj.828, 2011.

Ding, A. J., Fu, C. B., Yang, X. Q., Sun, J. N., Zheng, L. F., Xie, Y. N., Herrmann, E., Nie, W., Petäjä, T., Kerminen, V. M., and Kulmala, M.: Ozone and fine particle in the western Yangtze River Delta: an overview of 1 yr data at the SORPES station, Atmospheric Chemistry and Physics, 13(11), 5813-5830, doi:10.5194/acp-13-5813-2013, 2013.

Ding, A. J., Wang, T., Zhao, M., Wang, T. J., Li, Z. K.: Simulation of sea-land breezes and a discussion of their implications on the transport of air pollution during a multi-day ozone episode in the Pearl River Delta of China, Atmospheric Environment, 38(39):6737-6750, doi:10.5194/acpd-13-2835-2013, 2004.

Doherty, R. M., Wild, O., Shindell, D. T., Zeng, G., MacKenzie, I. A., Collins, W. J., Fiore, A. M., Stevenson, D. S., Dentener, F. J., Schults, M. G., Hess, P., Derwent, R. G., Keating, T. J.: Impacts of climate change on surface ozone and intercontinental

ozone pollution: A multi-model study, Journal of Geophysical Research Atmospheres, 118(9), 3744–3763, doi:10.1002/jgrd.50266, 2013.

Fu, J.S., Dong, X., Gao, Y.,Wong, D.C., Lam, Y.F. Sensitivity and linearity analysis of ozone in East Asia: the effects of domestic emission and intercontinental transport. J. AirWaste Manage. Assoc. 62, 1102–1114, 2012

Gao, W., Tie, X. X., Xu, J. M., Huang, R. J., Mao, X. Q., Zhou, G. Q., Chang, L. Y.: Long-term trend of O_3 in a mega City (Shanghai), China: Characteristics, causes, and interactions with precursors, Science of the Total Environment, 603–604,425–433, doi:10.1016/j.scitotenv.2017.06.099, 2017.

Jin, X. M., Holloway T., Spatial and temporal variability of ozone sensitivity over China observed from the Ozone Monitoring Instrument, Journal of Geophysical Research: Atmospheres, 120, 7229–7246, doi:10.1002/2015JD023250, 2015.

Li, J. F., Lu, K. D., Lv, W., Li, J., Zhong, L. J., Ou, Y. B., Chen, D. H., Huang, X., Zhang, Y. H.: Fast increasing of surface ozone concentrations in Pearl River Delta characterized by a regional air quality monitoring network during 2006–2011, Journal of Environmental Sciences, 26, 23–36, doi:10.1016/S1001-0742(13)60377-0, 2014.

Li, K., Jacob, D. J., Liao, H., Shen, L., Zhang, Q., Bates, K. H.: Anthropogenic drivers of 2013–2017 trends in summer surface ozone in China, Proceedings of the National Academy of Sciences of the United States of America, 116(2), 422-427, doi:10.1073/pnas.1812168116, 2018

Lin, M. Y., Fiore, A. M., Horowitz, L. W., Langford, A. O., Oltmans, S. J., Tarasick, D., and Rieder, H. E.: Climate variability modulates western US ozone air quality in spring via deep stratospheric intrusions, Nature Communications, 6(1), 7105-7105, doi:10.1038/ncomms8105, 2015.

Lu, X., Hong, J. Y., Zhang, L., Cooper, O. R., Schultz, M. G., Xu, X. B., Wang, T., Gao, M., Zhao, Y. H., Zhang, Y. H. Severe surface ozone pollution in China: A global perspective, Environmental Science & Technology Letters, 5, 487–494, doi:10.1021/acs.estlett.8b00366, 2018.

Lu, X., Zhang, L., Chen, Y., Zhou, M., Zheng, B., Li, K., Liu, Y., Lin, J., Fu, T.-M., and Zhang, Q.: Exploring 2016–2017 surface ozone pollution over China: source contributions and meteorological influences, Atmos. Chem. Phys., 19, 8339–8361, https://doi.org/10.5194/acp-19-8339-2019, 2019.

Ma, Z. Q., Xu, J., Quan, W. J., Zhang, Z. Y., Lin, W. L., and Xu, X. B.: Significant increase of surface ozone at a rural site, north of eastern China, Atmospheric Chemistry and Physics, 16(6), 3969–3977, doi:10.5194/acp-16-3969-2016, 2016.

North, G. R. , Bell, T. L. , Cahalan, R. F. , Moeng, F. J. Sampling errors in the estimation of empirical orthogonal functions. Monthly Weather Review, 110(7), 699-706, 1982

Pu, X., Wang, T. J., Huang, X., Melas, D., Zanis, P., Papanastasiou, D. K., Poupkou, A.: Enhanced surface ozone during the heat wave of 2013 in yangtze river delta region, china, Science of the Total Environment, 603, 807–816, https://doi.org/10.1016/j.scitotenv.2017.03.056, 2017.

Shi, C. Z., Wang, S. S., Liu, R., Zhou, R., Li, D. H., Wang, W. X., Li, Z. Q., Cheng, T. T., Zhou, B.: A study of aerosol optical properties during ozone pollution episodes in 2013 over Shanghai, China. Atmospheric Research, 153, 235–249, doi:10.1016/j.atmosres.2014.09.002, 2015.

Sun, L., Xue, L. K., Wang, T., Gao, J., Ding, A. J., Cooper, O. R., Lin, M. Y., Xu, P. J., Wang, Z., Wang, X. F., Wen, L., Zhu, Y. H., Chen, T. S., Yang, L. X., Wang, Y., Chen, J. M., and Wang, W. X.: Significant increase of summertime ozone at Mount Tai in Central Eastern China, Atmospheric Chemistry and Physics, 16, 10637-10650, doi:10.5194/acp-16-10637-2016, 2016.

The Ministry of Environmental Protection of China: Technical Regulation on Ambient Air Quality Index, China Environmental Science Press, China, 2012

Tong, L., Zhang, H. L., Yu, J., He, M. M., Xu N. B., Zhang, J. J., Qian F. Z., Feng J. Y., and Xiao, H.: Characteristics of surface ozone and nitrogen oxides at urban, suburban and rural sites in Ningbo, China, Atmospheric Research, 187: 57–68, https://doi.org/10.1016/j.atmosres.2016.12.006, 2017.

Wang, T., Ding, A., Gao, J., Wu, W. S.: Strong ozone production in urban plumes from Beijing, China, Geophysical Research Letters, 33(21), 320–337, doi:10.1029/2006GL027689, 2006.

Wang, T., Nie, W., Gao, J., Xue, L. K.: Air quality during the 2008 Beijing Olympics: secondary pollutants and regional impact. Atmospheric Chemistry and Physics, 10(16), 7603-7615, doi:10.5194/acp-10-7603-2010, 2010.

Wang, T., Xue, L. K., Brimblecombe, P., Lam, Y. F., Li, L., Zhang, L.: Ozone pollution in China: A review of concentrations, meteorological influences, chemical precursors, and effects, Science of The Total Environment, 575, 1582-1596, doi:10.1016/j.scitotenv.2016.10.081, 2017.

Wang, Y. X., Shen, L. L., Wu, S. L., Mlckley, L., He, J. W., and Hao, J. M.: Sensitivity of surface ozone over China to 2000–2050 global changes of climate and emissions, Atmospheric Environment, 75, 372–382, doi:10.1016/j.atmosenv.2013.04.045, 2013.

Wilks, D.S., 2011. Statistical Methods in the Atmospheric Sciences. Academic press.

Xiao, Z. , Wang, Z. , Pan, W. , Wang, Y. , Yang, S. Sensitivity of extreme temperature events to urbanization in the pearl river delta region. Asia-Pacific Journal of the Atmospheric Sciences., 2018

Xu, Z. , Huang, X. , Nie, W. , Chi, X. , Xu, Z. , Zheng, L. , et al. Influence of synoptic condition and holiday effects on vocs and ozone production in the Yangtze river delta region, china. Atmospheric Environment, S1352231017305496, 2017

Yang, Y., Liao, H., Li, J. P.: Impacts of the East Asian summer monsoon on interannual variations of summertime surface-layer ozone concentrations over China. Atmospheric Chemistry and Physics, 14:6867–6879, doi:10.5194/acp-14-6867-2014, 2014.

Yin, Z. C., Wang, H. J., and Guo, W. L.: Climatic change features of fog and haze in winter over North China and Huang-Huai Area, Sci. China. Earth. Sci., 58(8): 1370–1376, 2015.

Yin, Z. C., Wang, H. J., Li, Y. Y., Ma, X. H., Zhang, X. Y.: Links of Climate Variability among Arctic sea ice, Eurasia teleconnection pattern and summer surface ozone pollution in North China, Atmospheric Chemistry and Physics, 19, 3857–3871, https://doi.org/10.5194/acp-19-3857-2019, 2019.

Yue X, Unger, N., Harper, K., Xia, X. G., Liao, H., Zhu, T., Xiao J. F., Feng, Z. Z., and Li, J.: Ozone and haze pollution weakens net primary productivity in China, Atmospheric Chemistry and Physics, 17:6073–6089, doi:10.5194/acp-2016-1025, 2017.

Zhao, Z. J., Wang, Y. X.: Influence of the west pacific subtropical high on surface ozone daily variability in summertime over eastern china, Atmospheric Environment, 170, 197–204, https://doi.org/10.1016/j.atmosenv.2017.09.024, 2017.

Figures captions

Table 1. Correlation coefficients between the time series of PAT1 (PAT2) and the key indices of atmospheric circulations and meteorological conditions. "**" and "*" indicate that the correlation coefficients were above the 99% and 95% confidence level, respectively.

Figure 1. Distribution of the (a) mean values and (b) maximum values of MDA8 (Unit: μg/m³) at the observation sites in summer from 2015 to 2018. The black boxes in panels a and b indicated the locations of North China and Huanghuai region (NCH), North China (NC), Yangtze River Delta (YRD) and Pearl River Delta (PRD).

Figure ~~7~~2. Anomalies of the summer mean MDA8 (Unit: μg/m³) in 2015 (a), 2016 (b), 2017 (c) and 2018 (d), relative to the mean during 2015–2018. The black pluses indicate that the maximum MDA8 was larger than 265 μg/m³. The black boxes in panel b indicated the locations of NC, YRD and PRD, while that in panel d was the NCH area.

Figure ~~2~~3. Variations in MDA8 (Unit: μg/m³) of polluted cities from 2015 to 2018, including (a) Beijing (capital of China), Tianjin and Tangshan near the capital city; (b) Taiyuan, Weifang and Shijiazhuang in the south of NCH; (c) Shanghai and Nanjing in YRD; and (d) Zhongshan and Guangzhou in PRD. The cities in panels (a)-(d) were located from north to south and were illustrated in Figure S2. The horizontal dash lines indicated the value of 100 μg/m³ and 215 μg/m³.

Figure ~~3~~4. The first EOF pattern (PAT1: a, b) and second EOF pattern (PAT2: c, d) of MDA8 in summer from 2015 to 2018, including the spatial pattern (a, c) and the time coefficient (b, d). The black boxes in panels a and c are the selected North China and Huanghuai region (NCH), North China (NC), Yangtze River Delta (YRD) and Pearl River Delta (PRD). The EOF analysis were applied to the daily MDA8 anomalies at 868 stations to extract the relatively change features of the original data on the daily time-scale. The percentages on panel (b) and (d) were the variance contributions of the first and second EOF mode. The horizontal dash lines indicated one standard deviation, and the vertical ones separated the years.

Figure ~~4~~5. Composites of the MDA8 (Unit: μg/m³) for PAT1 (a, b) and PAT2 (c, d) in summer from 2015 to 2018. Panels (a) and (c) were composited when the time coefficient of EOF1 and EOF2 was greater than one standard deviation, while panels (b) and (d) were composited when the time coefficient was less than ~~—~~1 ×one standard deviation. The black box in panel a-b indicated the location of NCH, while those in panel c-d were the NH, YRD and PRD area.

Figure ~~5~~6. Differences of the daytime atmospheric circulations (i.e., PAT1P minus PAT1N). (a) Geopotential height at 850 hPa (Unit: 10gpm, contours) and surface air temperature (Unit: K, shading), (b) water vapor flux (Unit: $gs^{-1}cm^{-1}hpa^{-1}$~~kg*m/(kg*s)~~) at 850 hPa (arrows) and precipitation (Unit: mm, shading), (c) 100°E–120°E mean wind (Unit: m/s, arrows) and relative humidity (Unit: %, shading), (d) downward solar radiation at the surface (Unit:10^7 J/m^2, shading) and the sum of low and medium cloud cover (Unit: 1, contours). The white dots indicate that the shading was above the 95% confidence level. The green boxes in panels (a), (b) and (d) show the NCH region, and the black box in panel (a) indicates the location of the East Asia trough. The purple triangles in panel (a) indicated the data used to calculate the $WPSH_1$, while the red triangle represented the west ridge point of WPSH.

Figure ~~6~~7. Differences of the daytime atmospheric circulations (i.e., PAT2P minus PAT2N). (a) Geopotential height at 500 hPa (Unit: 10gpm, contours) and surface air temperature (Unit: K, shading), (b) water vapor flux (Unit: $gs^{-1}cm^{-1}hpa^{-1}$~~kg*m/(kg*s)~~) at 850 hPa (arrows) and precipitation (Unit: mm, shading), (c) 100°E–120°E mean wind (Unit: m/s, arrows) and relative humidity (Unit: %, shading), (d) downward solar radiation at the surface (Unit: 10^7J/m^2, shading) and the sum of low and medium cloud cover (Unit: 1, contours). The white dots indicate that the shading was above the 95% confidence level. The green boxes in panel (a), (b) and (d) are the NC and YRD regions, and the black box in panel (a) indicates the location of the East Asia trough. The purple triangles in panel (a) indicated the data used to calculate the $WPSH_2$.

Figure 8. The first (a, c, e, g) and second (b, d, f, h) EOF spatial patterns of MDA8 in summer in 2015 (a, b), 2016 (c, d), 2017, (e, f) and 2018(g, h). The percentage number in panels (a, c, e, g) and (b, d, f, h) are the variance contributions of the first and second EOF mode. The black boxes indicated the location of NCH, NH, YRD and PRD, respectively.

Figure 9. Variations in the MDA8 (Unit: μg/m³) of NC (black) and the YRD (blue) in 2016 (a) and 2018 (b). The MDA8 was calculated as an average for all available sites in the NC and the YRD regions.

~~**Figure 10.** Anomalies of summer mean daytime atmospheric circulations in 2016, with respect to the mean during 2015–2018. (a) Geopotential height at 500 hPa (Unit: 10gpm, contours) and surface air temperature (Unit: K, shading), (b) water vapor flux (Unit: kg*m/(kg*s)) at 850 hPa (arrows) and precipitation (Unit: 0.1mm, shading), (c) 100°E–120°E mean wind (Unit: m/s, arrows) and relative humidity (Unit: %, shading), (d) downward solar radiation at the surface (Unit: 10^4J/m^2, shading) and the sum of low and medium cloud cover (Unit: 1, contours). The green boxes in panel (a), (b) and (d) are the NC and YRD regions. The white dots indicate that the shading was above the 95% confidence level.~~

~~**Figure 11.** Anomalies of summer mean daytime atmospheric circulations in 2018 with respect to the mean during 2015–2018. (a) Geopotential height at 850 hPa (Unit: 10gpm, contours) and surface air temperature (Unit: K, shading), (b) water vapor flux (Unit: kg*m/(kg*s)) at 850 hPa (arrows) and precipitation (Unit: 0.1mm, shading), (c) 100°E–120°E mean wind (Unit: m/s, arrows) and relative humidity (Unit: %, shading), (d) downward solar radiation at the surface (Unit: 10^4J/m^2, shading) and the sum of low and medium cloud cover (Unit: 1, contours). The green boxes in panels (a), (b) and (d) show the NCH region. The white dots indicate that the shading was above the 95% confidence level.~~

Table 1. Correlation coefficients between the time series of PAT1 (PAT2) and the key indices of atmospheric circulations and meteorological conditions. "**" and "*" indicate that the correlation coefficients were above the 99% and 95% confidence level, respectively.

PAT1	**$MDA8_1$**	**EAT_1**	**$WPSH_1$**	**Pre_1**	**SAT_1**	**SSR_1**
	0.97^{**}	0.28^{**}	0.39^{**}	-0.44^{**}	0.14^{**}	0.64^{**}
PAT2	**$MDA8_2$**	**EAT_2**	**$WPSH_2$**	**Pre_2**	**SAT_2**	**SSR_2**
	0.77^{**}	0.30^{**}	0.32^{**}	-0.49^{**}	0.18^{**}	0.65^{**}

$MDA8_1$ is the NCH-area averaged MDA8, while the $MDA8_2$ is the MDA8 difference between NC and YRD. EAT_1 and EAT_2 indicate the intensity of the East Asia deep trough and were calculated as the mean –Z850 shown in the black boxes in Figure 5 and Figure 6, respectively. $WPSH_1$ ($Z500_{(125^0E,\ 20^0N)} - Z500_{(125^0E,\ 30^0N)}$) and $WPSH_2$ ($Z500_{(110^0E,\ 20^0N)} - Z500_{(110^0E,\ 30^0N)}$) represents the location of WPSH. Pre_1, SAT_1 and SSR_1 were calculated as the NCH-area averaged precipitation, SAT and downward solar radiation at the surface, respectively. Pre_2, SAT_2 and SSR_2 are the differences in the NC- and YRD-area averaged precipitation, SAT and downward solar radiation at the surface, respectively.

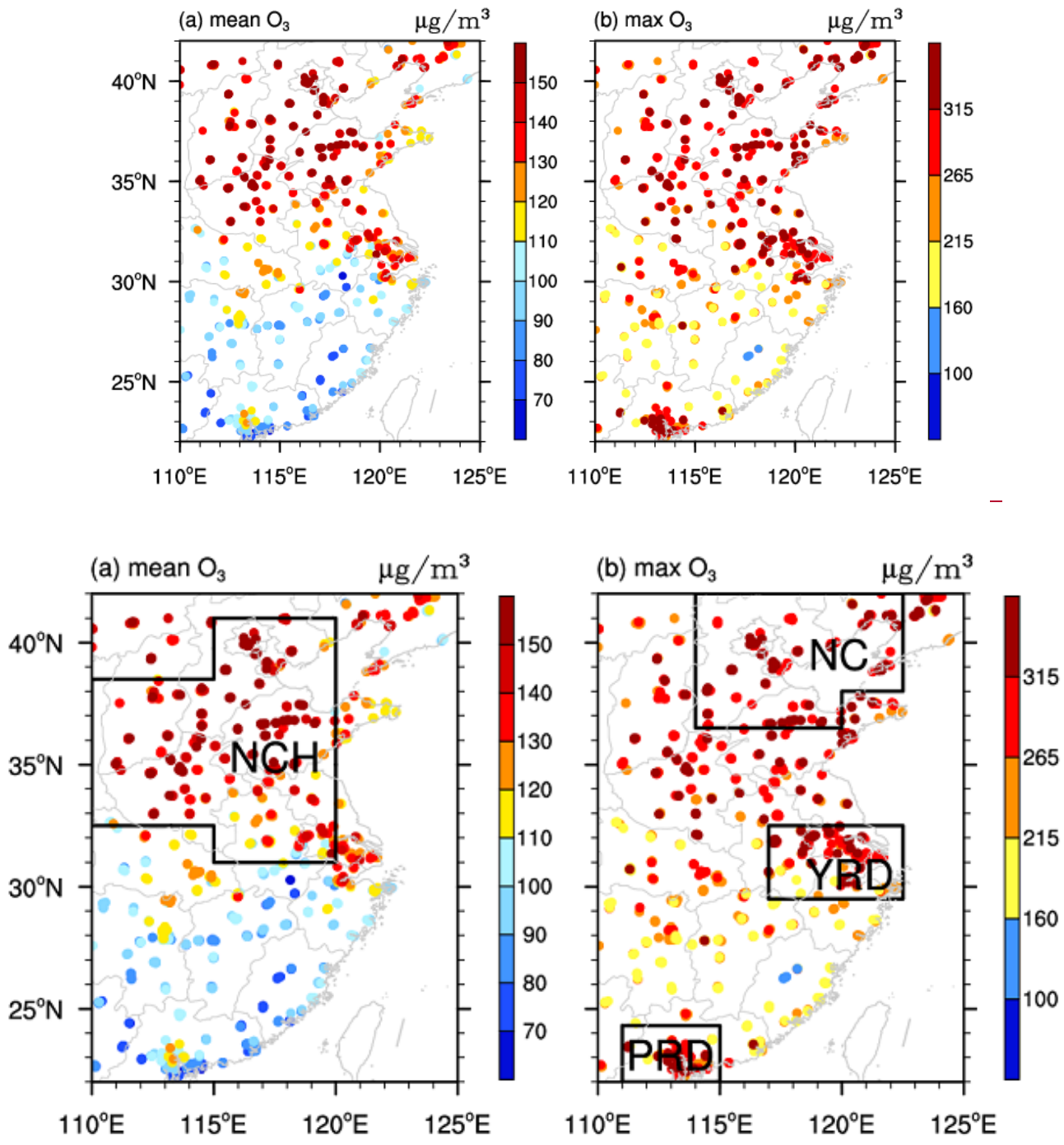

Figure 1. Distribution of the (a) mean values and (b) maximum values of MDA8 (Unit: μg/m³) at the observation sites in summer from 2015 to 2018. The black boxes in panels a and b indicated the locations of North China and Huanghuai region (NCH), North China (NC), Yangtze River Delta (YRD) and Pearl River Delta (PRD).

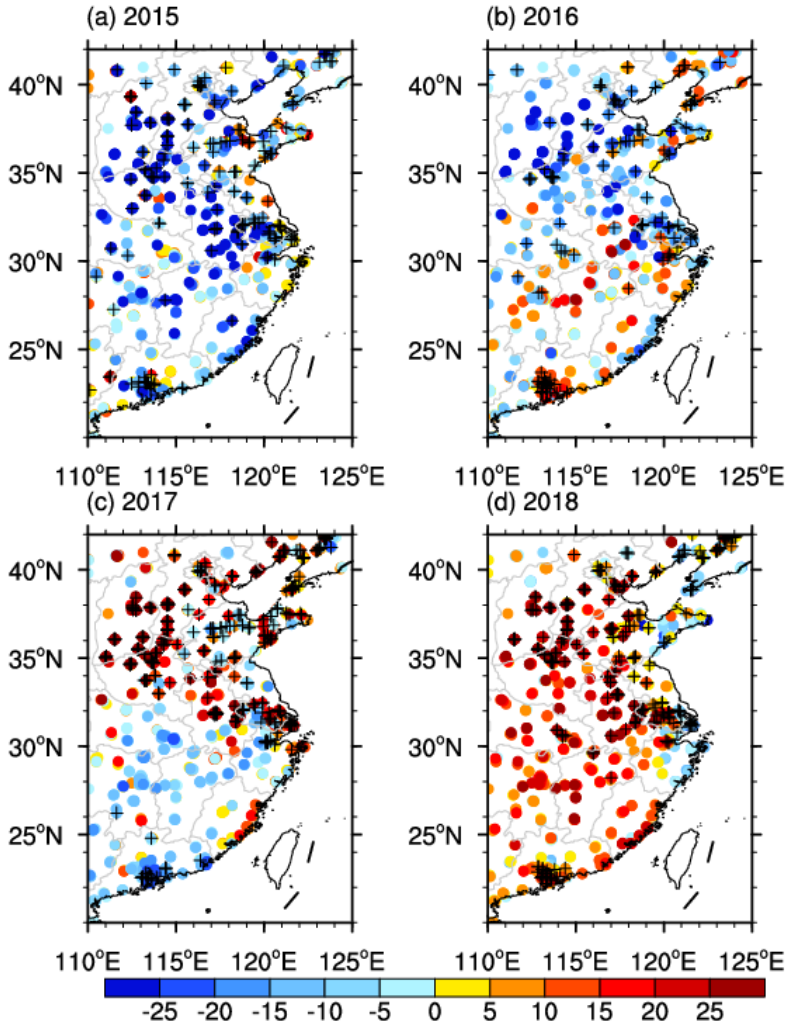
(a) 2015
(b) 2016
(c) 2017
(d) 2018
40°N
35°N
30°N
25°N
110°E
115°E
120°E
125°E
-25
-20
-15
-10
-5
0
5
10
15
20
25

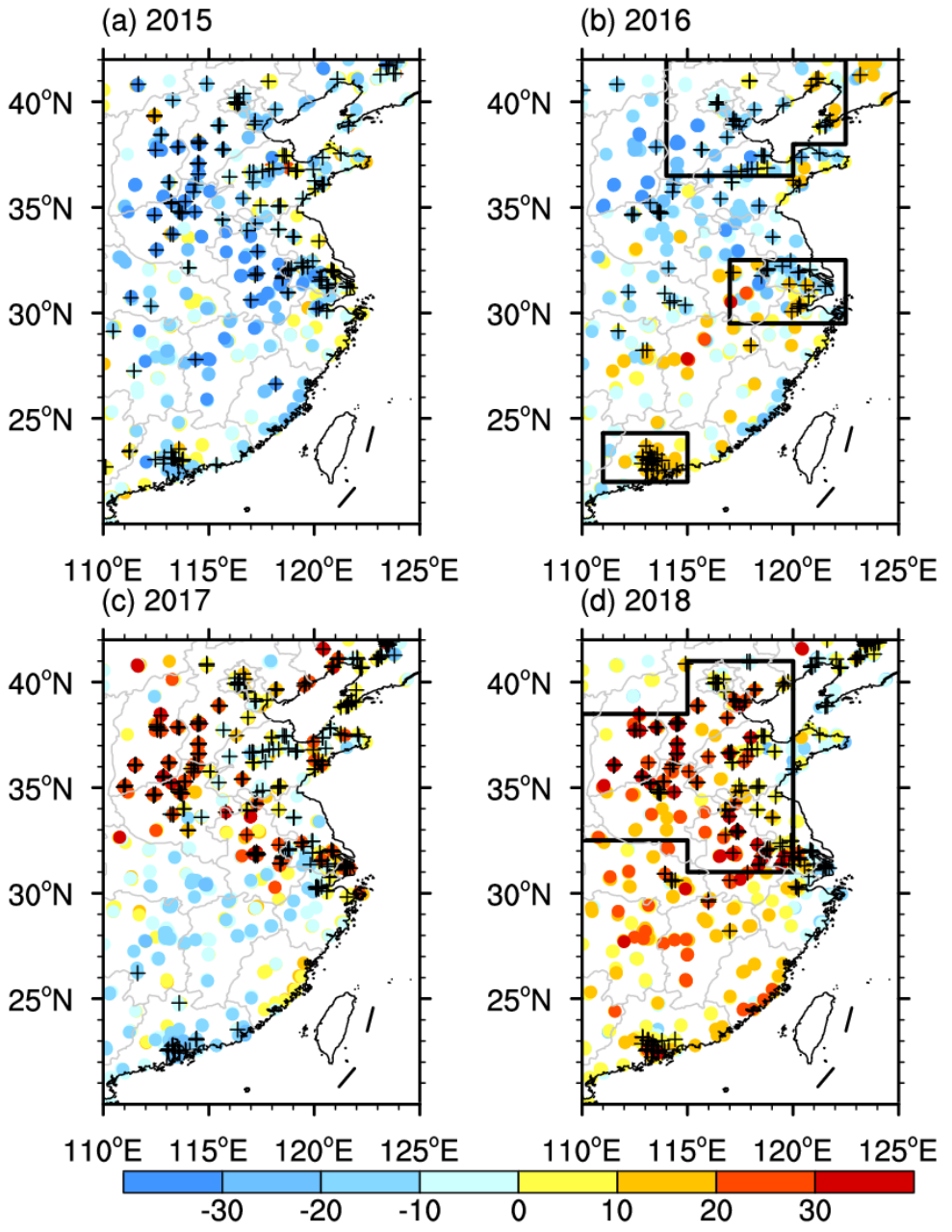

Figure ~~7~~2. Anomalies of the summer mean MDA8 (Unit: μg/m³) in 2015 (a), 2016 (b), 2017 (c) and 2018 (d), relative to the mean during 2015–2018. The black pluses indicate that the maximum MDA8 was larger than 265 μg/m³. The black boxes in panel b indicated the locations of NC, YRD and PRD, while that in panel d was the NCH area.

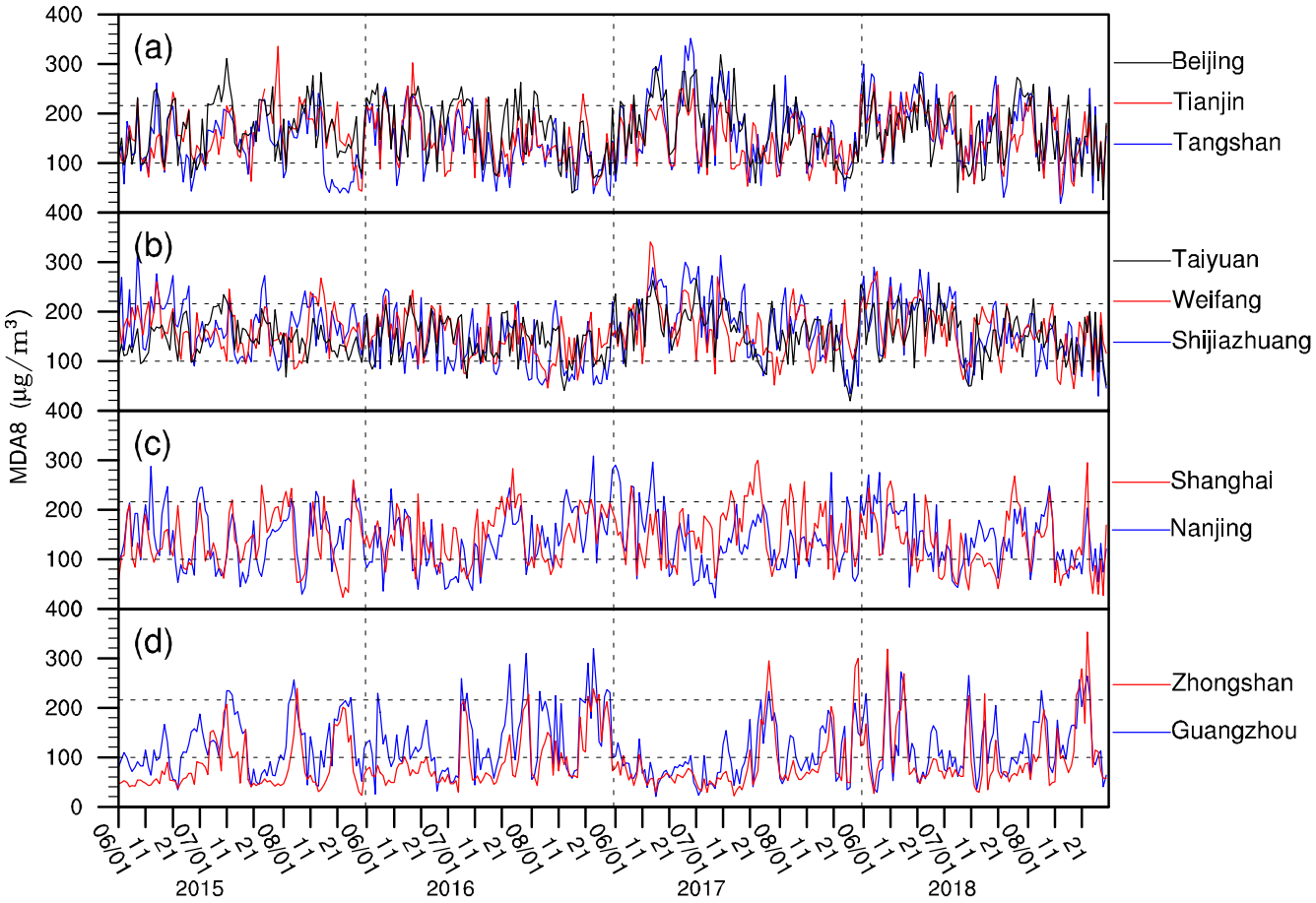

Figure ~~2~~3. Variations in MDA8 (Unit: μg/m³) of polluted cities from 2015 to 2018, including (a) Beijing (capital of China), Tianjin and Tangshan near the capital city; (b) Taiyuan, Weifang and Shijiazhuang in the south of NCH; (c) Shanghai and Nanjing in YRD; and (d) Zhongshan and Guangzhou in PRD. The cities in panels (a)-(d) were located from north to south and were illustrated in Figure S2. The horizontal dash lines indicated the value of 100 μg/m³ and 215 μg/m³.

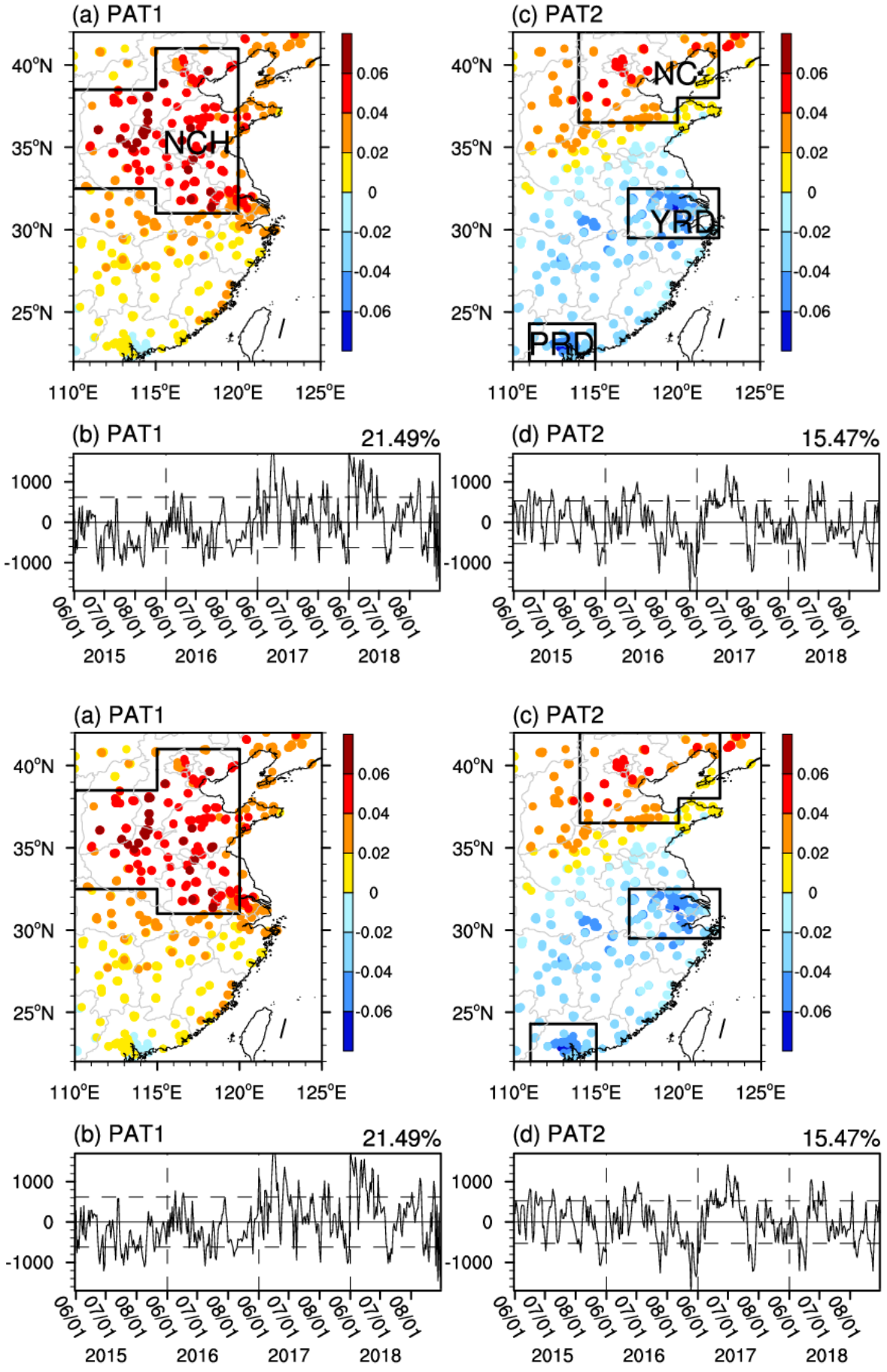

(a) PAT1
(c) PAT2
(b) PAT1
21.49%
(d) PAT2
15.47%

Figure ~~3~~4. The first EOF pattern (PAT1: a, b) and second EOF pattern (PAT2: c, d) of MDA8 in summer from 2015 to 2018, including the spatial pattern (a, c) and the time coefficient (b, d). The black boxes in panels a and c are the selected North

China and Huanghuai region (NCH), North China (NC), Yangtze River Delta (YRD) and Pearl River Delta (PRD). The EOF analysis were applied to the daily MDA8 anomalies at 868 stations to extract the relatively change features of the original data on the daily time-scale. The percentages on panel (b) and (d) were the variance contributions of the first and second EOF mode. The horizontal dash lines indicated one standard deviation, and the vertical ones separated the years.

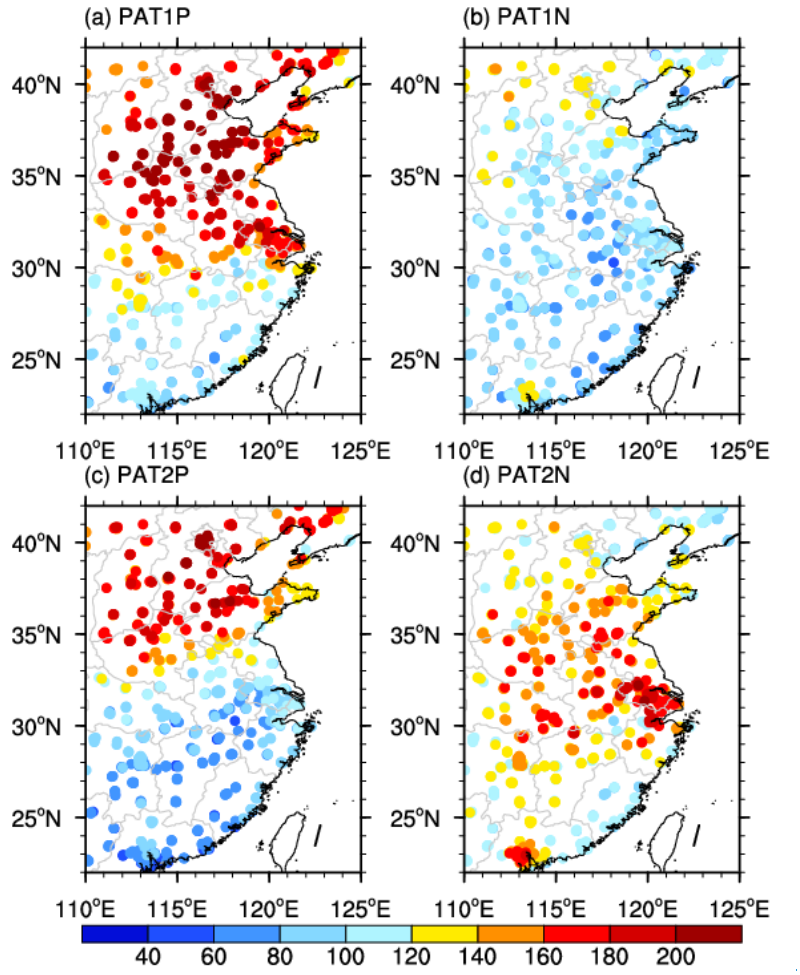

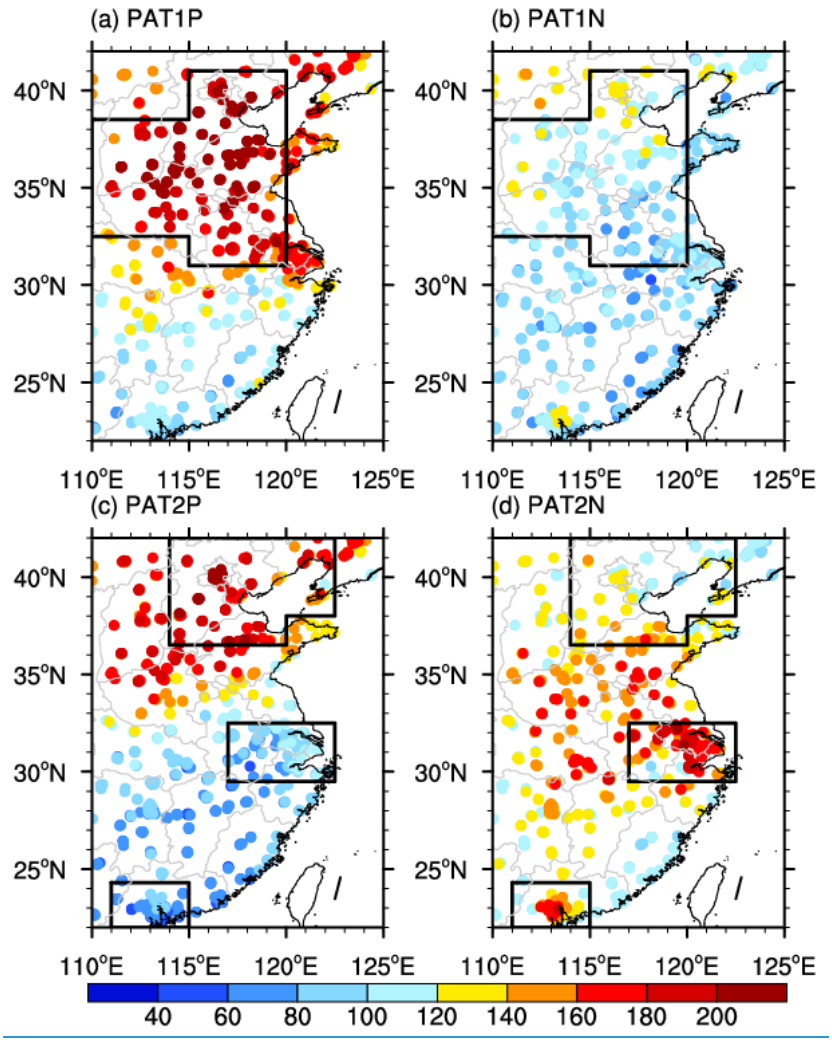

Figure 45. Composites of the MDA8 (Unit: μg/m³) for PAT1 (a, b) and PAT2 (c, d) in summer from 2015 to 2018. Panels (a) and (c) were composited when the time coefficient of EOF1 and EOF2 was greater than one standard deviation, while panels (b) and (d) were composited when the time coefficient was less than −1 ×one standard deviation. The black box in panel a-b indicated the location of NCH, while those in panel c-d were the NH, YRD and PRD area.

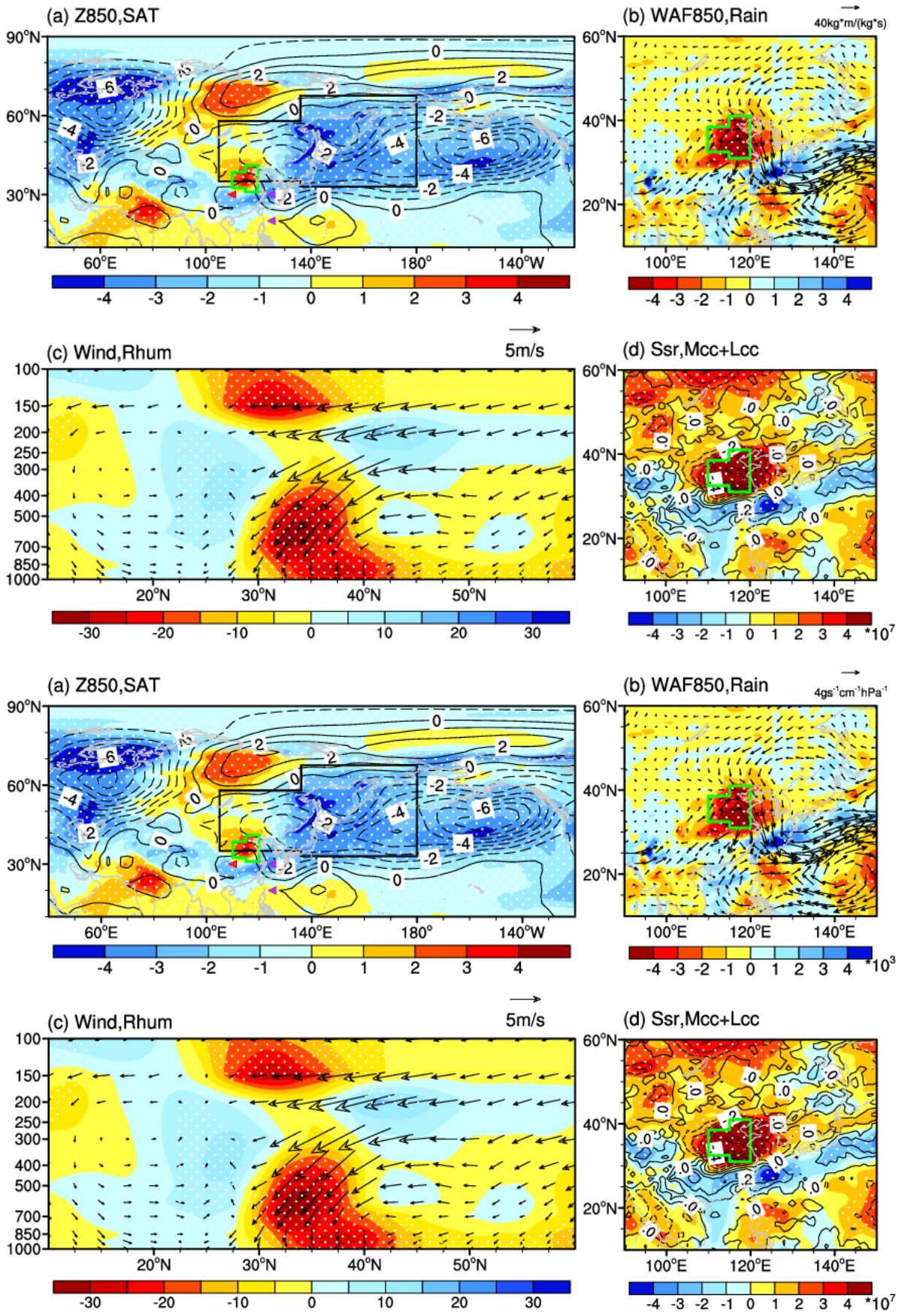

Figure ~~5~~6. Differences of the daytime atmospheric circulations (i.e., PAT1P minus PAT1N). (a) Geopotential height at 850 hPa (Unit: 10gpm, contours) and surface air temperature (Unit: K, shading), (b) water vapor flux (Unit: gs^{-1}cm^{-1}hpa^{-1}~~kg*m/(kg*s)~~) at 850 hPa (arrows) and precipitation (Unit: mm, shading), (c) 100°E–120°E mean wind (Unit: m/s, arrows) and relative humidity (Unit: %, shading), (d) downward solar radiation at the surface (Unit:10^7 J/m^2, shading)

and the sum of low and medium cloud cover (Unit: 1, contours). The white dots indicate that the shading was above the 95% confidence level. The green boxes in panels (a), (b) and (d) show the NCH region, and the black box in panel (a) indicates the location of the East Asia trough. The purple triangles in panel (a) indicated the data used to calculate the $WPSH_1$, while the red triangle represented the west ridge point of WPSH.

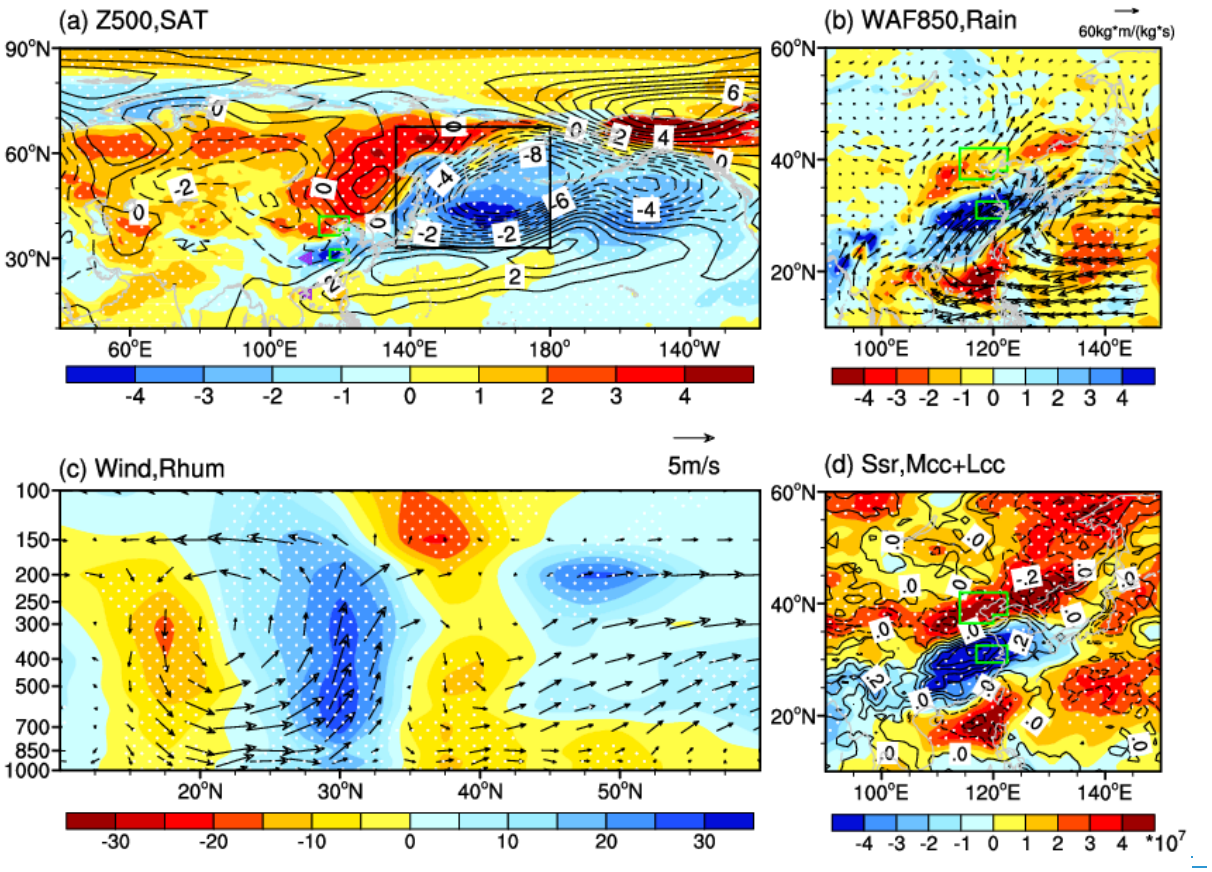

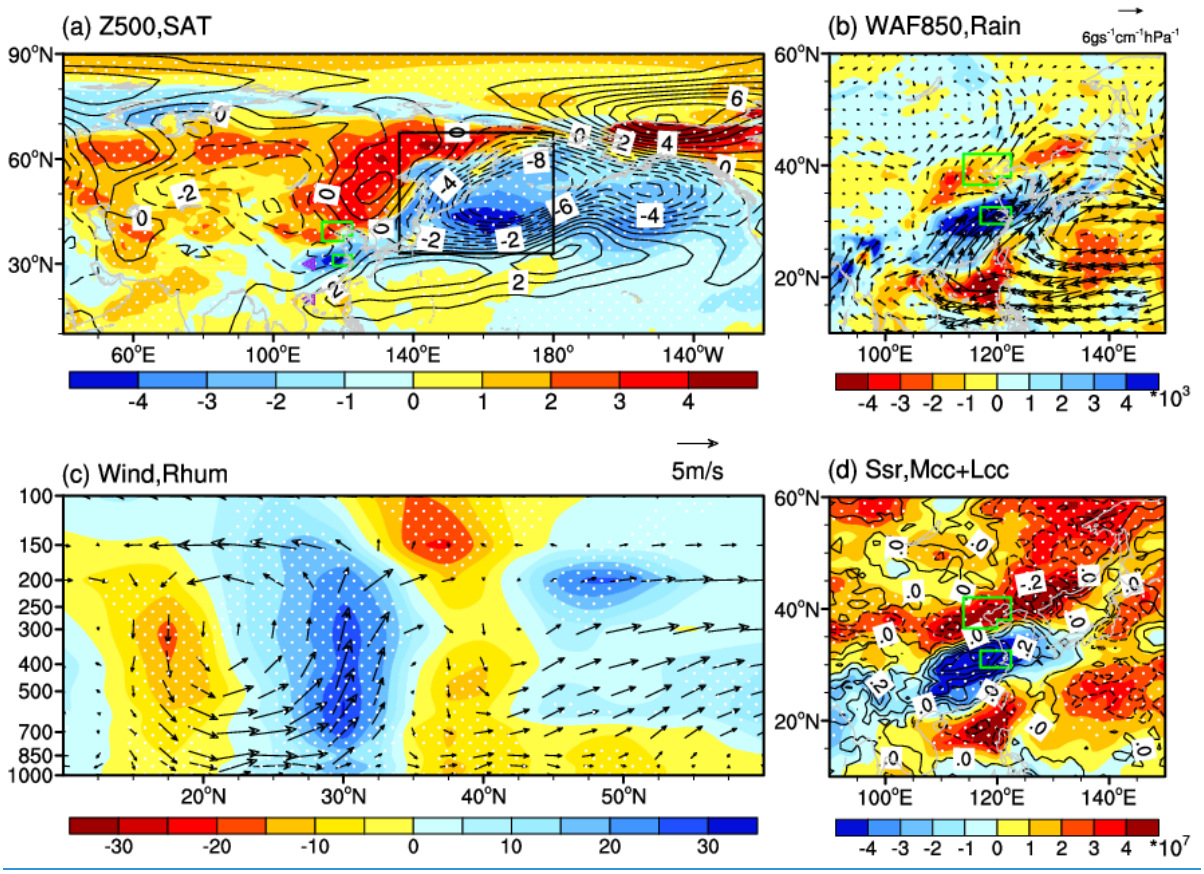

Figure ~~6~~7. Differences of the daytime atmospheric circulations (i.e., PAT2P minus PAT2N). (a) Geopotential height at 500 hPa (Unit: 10gpm, contours) and surface air temperature (Unit: K, shading), (b) water vapor flux (Unit: $gs^{-1}cm^{-1}hpa^{-1}$~~kg*m/(kg*s)~~) at 850 hPa (arrows) and precipitation (Unit: mm, shading), (c) 100°E–120°E mean wind (Unit: m/s, arrows) and relative humidity (Unit: %, shading), (d) downward solar radiation at the surface (Unit: $10^7 J/m^2$, shading) and the sum of low and medium cloud cover (Unit: 1, contours). The white dots indicate that the shading was above the 95% confidence level. The green boxes in panel (a), (b) and (d) are the NC and YRD regions, and the black box in panel (a) indicates the location of the East Asia trough. The purple triangles in panel (a) indicated the data used to calculate the $WPSH_2$.

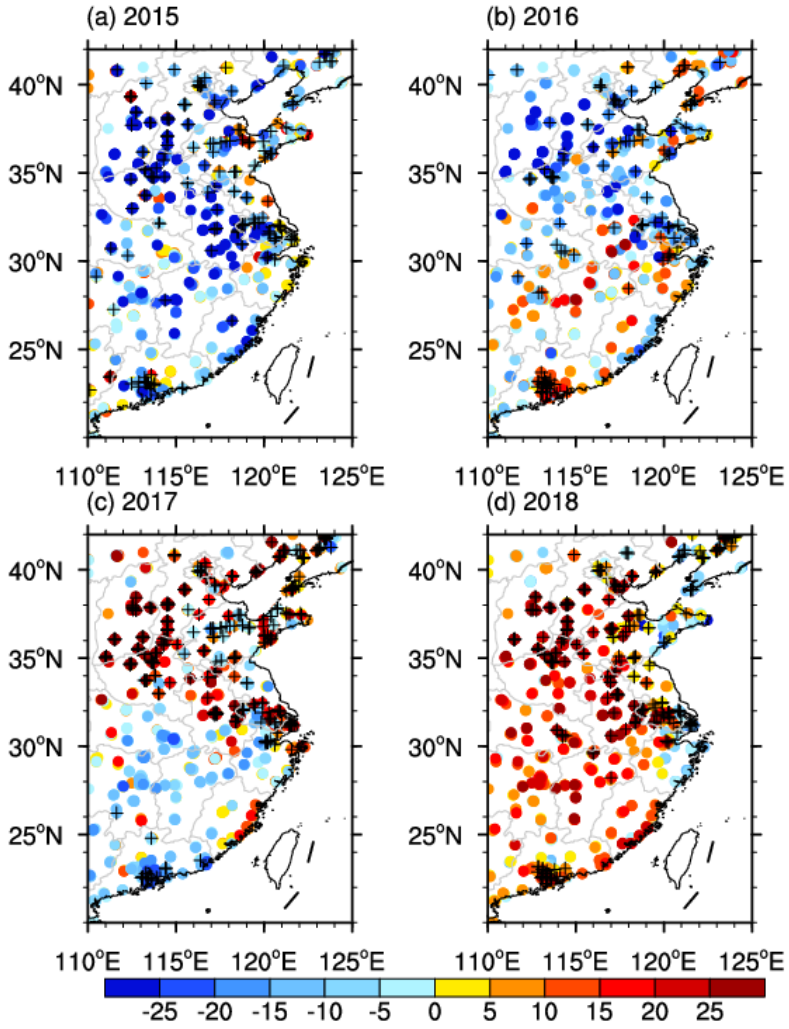

~~**Figure 7.** Anomalies of the summer mean MDA8 (Unit: μg/m³) in 2015 (a), 2016 (b), 2017 (c) and 2018 (d), relative to the mean during 2015–2018. The black pluses indicate that the maximum MDA8 was larger than 265 μg/m³.~~

585

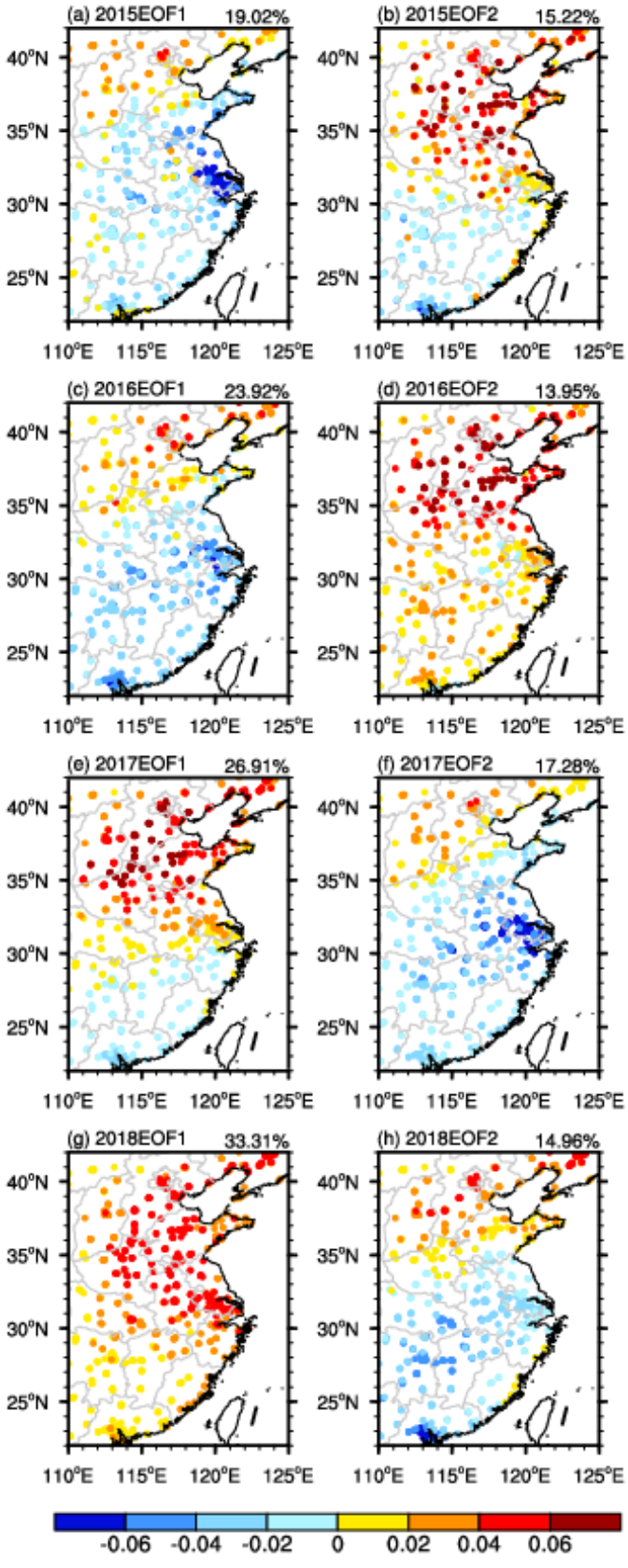
(a) 2015EOF1 19.02%
(b) 2015EOF2 15.22%
(c) 2016EOF1 23.92%
(d) 2016EOF2 13.95%
(e) 2017EOF1 26.91%
(f) 2017EOF2 17.28%
(g) 2018EOF1 33.31%
(h) 2018EOF2 14.96%
40°N
35°N
30°N
25°N
110°E 115°E 120°E 125°E
-0.06 -0.04 -0.02 0 0.02 0.04 0.06

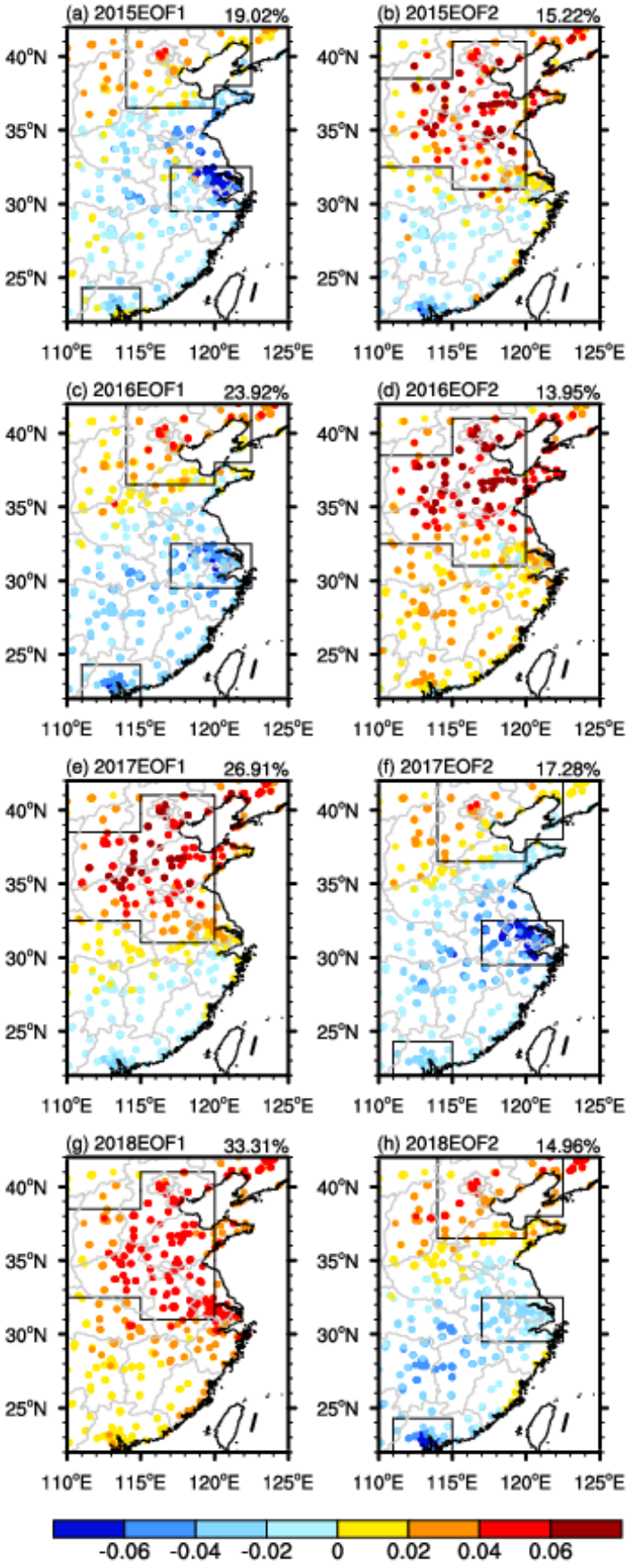

Figure 8. The first (a, c, e, g) and second (b, d, f, h) EOF spatial patterns of MDA8 in summer in 2015 (a, b), 2016 (c, d), 2017, (e, f) and 2018(g, h). The percentage number in panels (a, c, e, g) and (b, d, f, h) are the variance contributions of the first and second EOF mode. The black boxes indicated the location of NCH, NH, YRD and PRD, respectively.

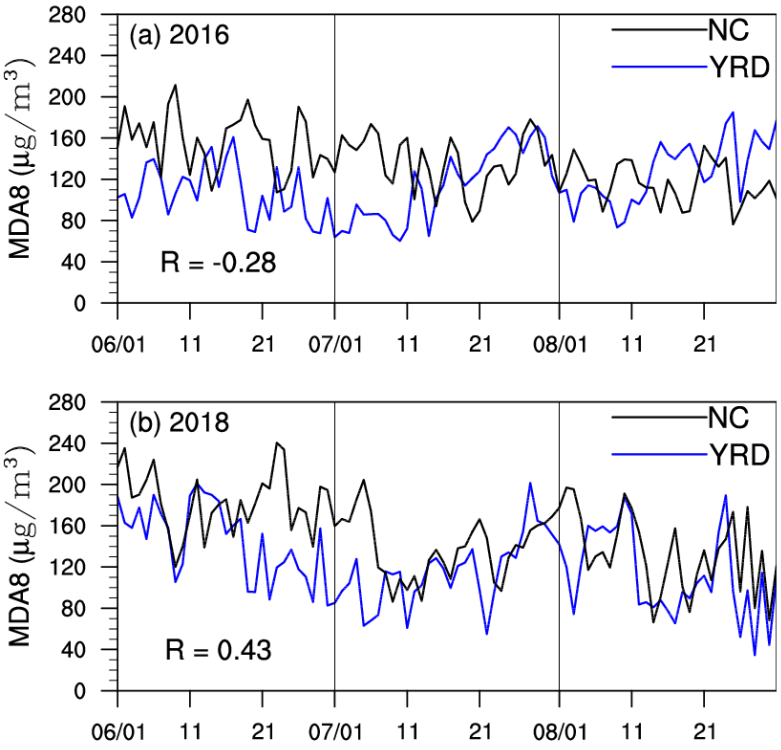

Figure 9. Variations in the MDA8 (Unit: μg/m³) of NC (black) and the YRD (blue) in 2016 (a) and 2018 (b). The MDA8 was calculated as an average for all available sites in the NC and the YRD regions.

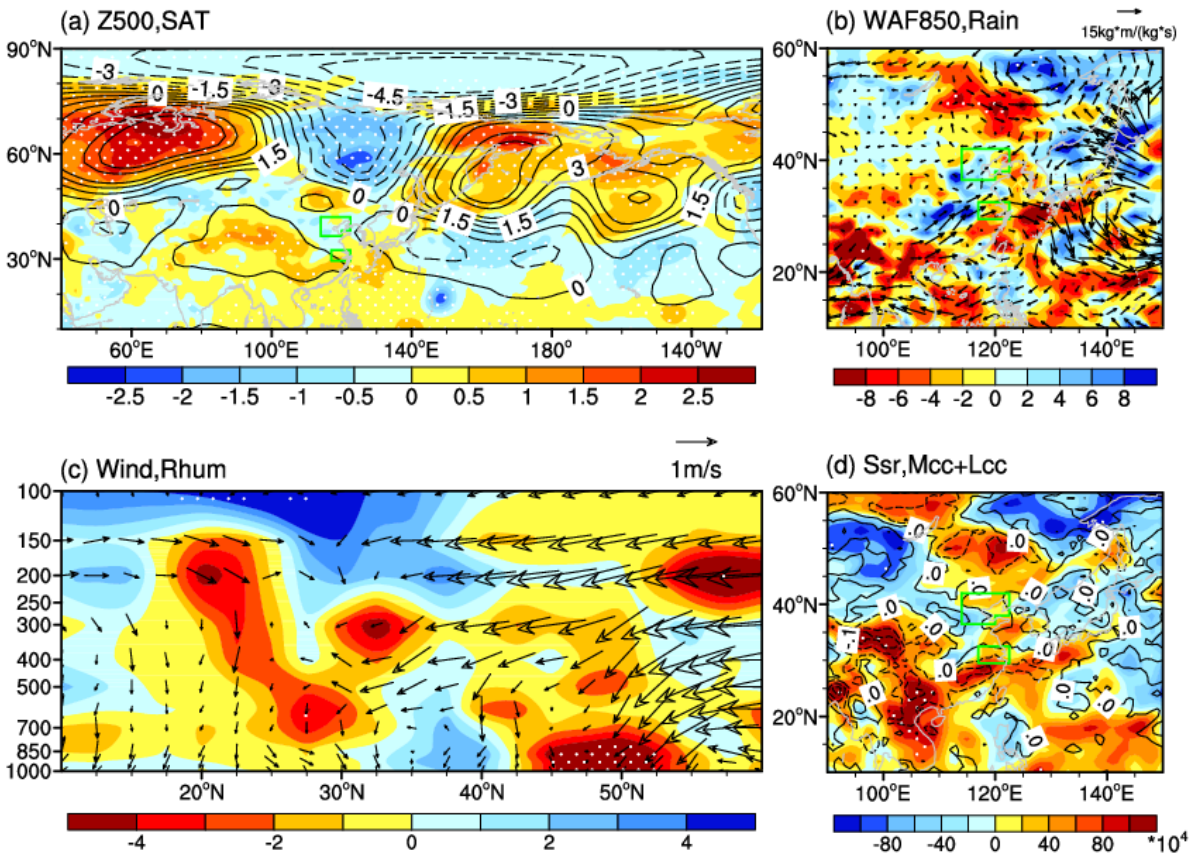

~~**Figure 10.** Anomalies of summer mean daytime atmospheric circulations in 2016, with respect to the mean during 2015–2018. (a) Geopotential height at 500 hPa (Unit: 10gpm, contours) and surface air temperature (Unit: K, shading), (b) water vapor flux (Unit: kg*m/(kg*s)) at 850 hPa (arrows) and precipitation (Unit: 0.1mm, shading), (c) 100°E–120°E mean wind (Unit: m/s, arrows) and relative humidity (Unit: %, shading), (d) downward solar radiation at the surface (Unit: 10^4J/m^2,~~

shading) and the sum of low and medium cloud cover (Unit: 1, contours). The green boxes in panel (a), (b) and (d) are the NC and YRD regions. The white dots indicate that the shading was above the 95% confidence level.

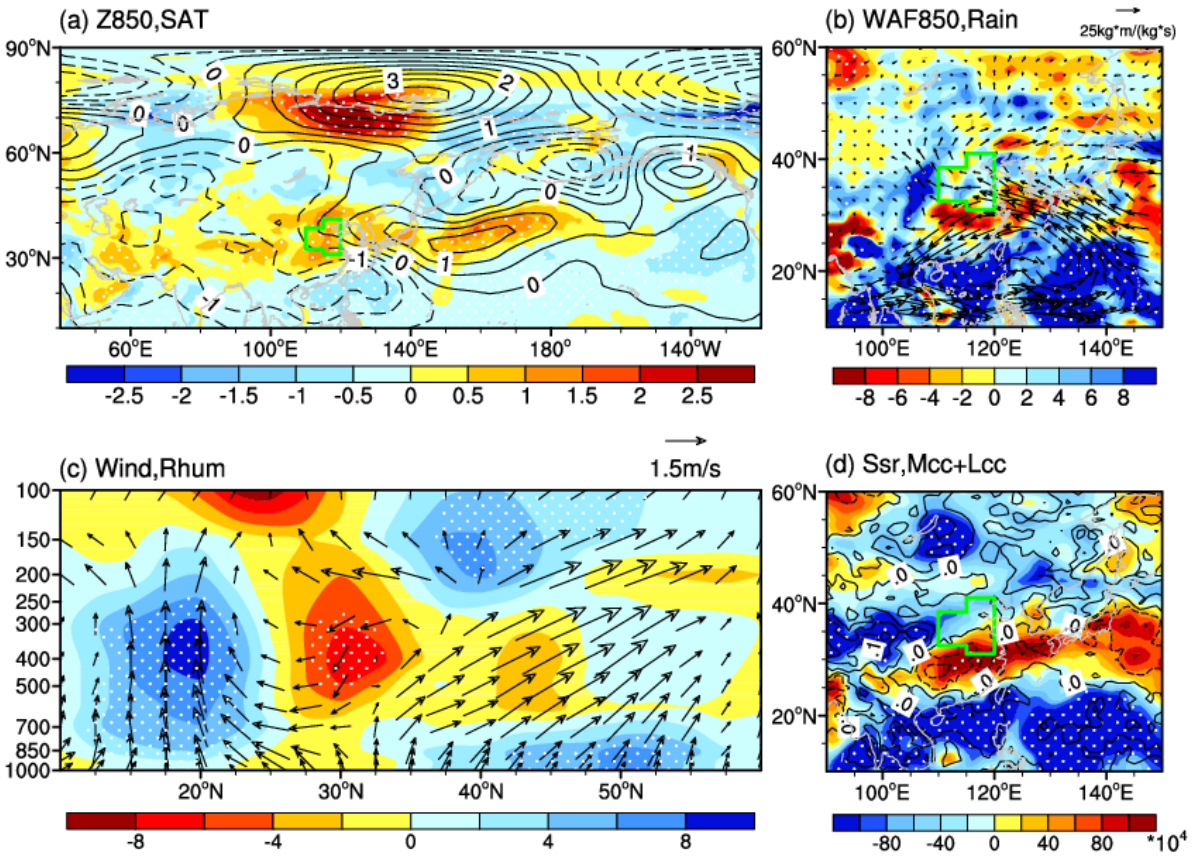

Figure 11. Anomalies of summer mean daytime atmospheric circulations in 2018 with respect to the mean during 2015–2018. (a) Geopotential height at 850 hPa (Unit: 10gpm, contours) and surface air temperature (Unit: K, shading), (b) water vapor flux (Unit: kg*m/(kg*s)) at 850 hPa (arrows) and precipitation (Unit: 0.1mm, shading), (c) 100°E–120°E mean wind (Unit: m/s, arrows) and relative humidity (Unit: %, shading), (d) downward solar radiation at the surface (Unit: 10^4J/m^2, shading) and the sum of low and medium cloud cover (Unit: 1, contours). The green boxes in panels (a), (b) and (d) show the NCH region. The white dots indicate that the shading was above the 95% confidence level.